

Permafrost thaw and implications for the fate and transport of tritium in the Canadian north

Matthew J. Bond*, Jamie Carr

Environmental Sciences Branch, Canadian Nuclear Laboratories, 286 Plant Road, Chalk River, Ontario, K0J 1J0, Canada

ARTICLE INFO

Keywords:

Permafrost degradation
Tritium
Sub-arctic contaminant cycling
Arctic radioecology
Climate change
Radionuclides

ABSTRACT

Layers of permafrost developed during the 1950s and 1960s incorporated tritium from the atmosphere that originated from global nuclear weapons testing. In regions underlain by substantial permafrost, this tritium has been effectively trapped in ice since it was deposited and subject to radioactive decay alone, which has substantially lengthened its environmental half-life compared to areas with little or no permafrost where the weapons-test era precipitation has been subject to both decay and hydrodynamic dispersion. The Arctic is warming three times faster than other parts of the world, with northern regions incurring some of the most pronounced effects of climate change, resulting in permafrost degradation. A series of 23 waterbodies across the Canadian sub-Arctic spanning the continuous, discontinuous and isolated patches permafrost zones in northern Manitoba, Northwest Territories and Labrador were sampled. Surface water and groundwater seepage samples were collected from each lake and analyzed for tritium, stable isotopes ($\delta^{18}\text{O}$ and $\delta^2\text{H}$) and general water chemistry characteristics. Measured tritium was significantly higher in surface waters (SW) and groundwater seepage (GW) in water bodies located in the sporadic discontinuous (64 ± 15 TU in SW and 52 ± 9 TU in GW) and extensive discontinuous (53 ± 7 TU in SW and 61 ± 7 TU in GW) permafrost regions of the Northwest Territories than in regions underlain by continuous permafrost in northern Manitoba (< 12 TU in both SW and GW) or those within isolated patches of permafrost in Labrador (16 ± 2 TU in SW and 21 ± 4 TU in GW). The greatest tritium enrichment (up to 128 TU) was observed in lakes near Jean Marie River in the Mackenzie River valley, a region known to be experiencing extensive permafrost degradation. These results demonstrate significant permafrost degradation in the central Mackenzie River basin and show that tritium is becoming increasingly mobile in the sub-Arctic environment—at concentrations higher than expected—as a result of a warming climate. A better understanding of the cycling of tritium in the environment will improve our understanding of Arctic radioecology under changing environmental conditions.

1. Introduction

1.1. Permafrost degradation in response to climate change

Permafrost occupies about 50% of Canada's land area (Smith and Burgess, 2004) and plays an important role in many hydrological, geochemical and ecological processes in these regions. Permafrost, however, is particularly sensitive to climate change and a number of recent studies have shown that permafrost is warming and degrading, resulting in a deepening of the active layer (Åkerman and Johansson, 2008; Smith et al., 2009; Jorgenson et al., 2012; Quinton and Baltzer, 2013). Recent studies have identified a general increasing trend in the active layer thickness in many regions, including Russia (Anisimov and Reneva, 2006), Tibet (Wu et al., 2010), northern Europe (Åkerman and

Johansson, 2008), Alaska (Jafarov et al., 2013) and the Canadian Arctic (Smith et al., 2009; Quinton and Baltzer, 2013). Widespread warming in permafrost regions will result in substantial changes in terrestrial hydrology (Woo et al., 2008), vegetation composition (Danby and Hik, 2007), landscape topography (Rowland et al., 2010), methane fluxes (Christensen et al., 2004), ecosystem function (Grosse et al., 2016) and fate and transport of contaminants (Klaminder et al., 2008, 2010; Rydberg et al., 2010; Schuster et al., 2018), including radionuclides (AMAP, 2011).

In the northern portion of the permafrost region, permafrost is spatially continuous and may be several hundred metres thick, typically persisting at ground temperatures less than -5°C (Heginbottom et al., 1995). Farther south, permafrost conditions become discontinuous and patchy and the permafrost layer is only several metres thick, persisting

* Corresponding author.

E-mail address: matthew.bond@cnl.ca (M.J. Bond).

at ground temperatures around -2°C to 0°C (Smith, 2011; Quinton and Baltzer, 2013). Such conditions make permafrost in these discontinuous zones sensitive to climate warming and many regions are experiencing extensive permafrost degradation (Payette et al., 2004; Camill, 2005; Smith, 2011). Camill (2005) found that permafrost thaw rates have accelerated significantly across the Canadian sporadic and discontinuous permafrost zones over the past 50 years, with thaw rates increasing by 200–300% since the 1940s. Overall, the area of near-surface permafrost in the northern hemisphere is projected to decline by 20% relative to today's area by 2040, and could retract by as much as 60% by 2080 under a scenario of high greenhouse gas emissions (AMAP, 2017).

1.2. Permafrost degradation and mobilization of weapons-era tritium

The extent to which thawing permafrost will change the fate and transport of contaminants in the Canadian north remains a significant gap in our knowledge of how ecosystems will respond to climate warming (Vonk et al., 2015). The long-range transport of contaminants has brought elevated concentrations of pesticides, metals and radionuclides to the Canadian north, which are then deposited into various compartments of the environment by precipitation and atmospheric deposition (Barrie et al., 1992). Permafrost can accumulate atmospherically-derived contaminants as they are washed out of the atmosphere during precipitation events and act as a long-term storage unit for contaminants and other solutes (Schindler and Smol, 2006; Grannas et al., 2013; Vonk et al., 2015). However, climate warming will likely disrupt this sequestration of contaminants in permafrost soils, and permafrost thaw may result in increased mobility of contaminants and other solutes from catchment soils to surface waters due to accelerated soil/peat erosion, increased hydrological connectivity and increased runoff leading to exposure of soluble contaminants (Dyke, 2001; Fortier et al., 2007; Klaminder et al., 2008, 2010; Rydberg et al., 2010; Gordon et al., 2016; Bouchard et al., 2017).

Most of the studies on the interactions between contaminants and permafrost thaw have focussed on petroleum products, persistent organic pollutants and metals such as mercury and lead (Vonk et al., 2015; Schuster et al., 2018). However, relatively little attention has been paid to the effects of permafrost thaw on the fate and transport of radionuclides such as tritium (${}^3\text{H}$) in the northern environment. Tritium is a naturally occurring radioisotope of hydrogen with a half-life ($t_{1/2}$) of 12.32 years. Tritium is directly incorporated into the water molecule, making it highly mobile in the environment and a useful marker for hydrological studies (Clark and Fritz, 1997). Atmospheric nuclear weapons testing, which occurred from about 1945 to 1980 and peaked in the early 1960s, led to elevated tritium emissions in the atmosphere around the globe (Clark and Fritz, 1997). The northern hemisphere received the bulk of these tritium emissions, with the sub-Arctic and Arctic receiving the highest loads (Aarkrog, 1994, Fig. 1a). For example, tritium concentrations in precipitation peaked at $\sim 10,000$ tritium units (T.U.; ~ 1000 times background) in Whitehorse, Yukon, and reached 6960 T.U. (~ 696 times background) in Fort Smith, Northwest Territories, both occurring in 1963 (IAEA and WMO, 2017). Fig. 1 shows a snapshot of June 1963 tritium fallout around the northern hemisphere and the distribution of different permafrost zones across the Canadian north. Since the 1960s, tritium concentrations in precipitation and most surface waters have declined exponentially and are now close to natural levels (Clark and Fritz, 1997; IAEA and WMO, 2017). This exponential decline in tritium concentrations in surface waters is far greater than that accounted for by radiological decay alone, owing to hydrodynamic dispersion and mixing with waters not enriched by weapons-era tritium. In many permafrost regions, however, it is anticipated that the influence of hydrodynamic dispersion on tritium concentration would be minimal because (i) precipitation is incorporated into permafrost relatively quickly (Woo, 2012) and (ii) in flat, peat- and bog-dominated permafrost landscapes, hydraulic

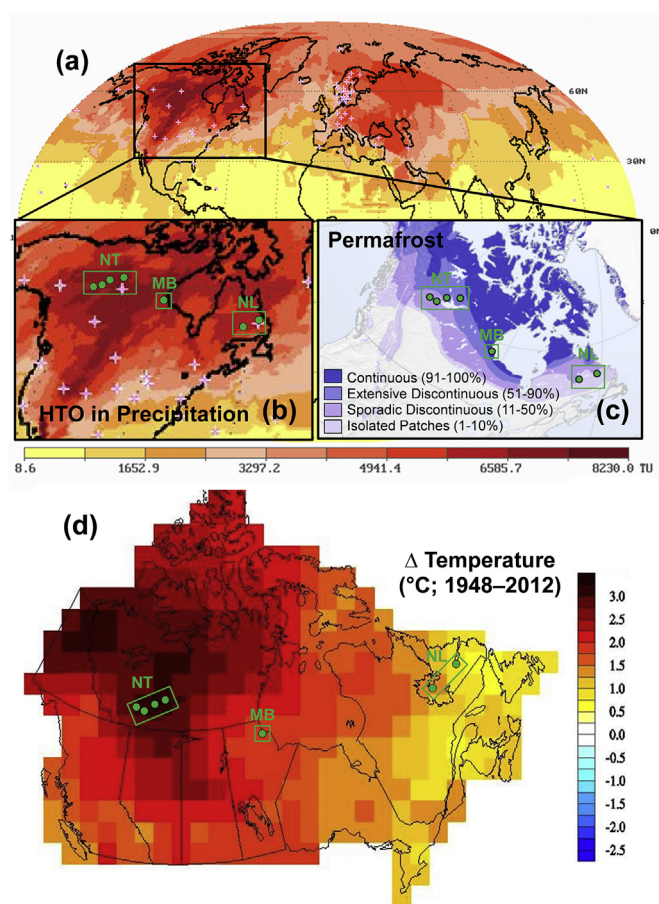


Fig. 1. (a) Tritium concentrations in precipitation in June 1963 at the global scale (from Aggarwal (2016) using the GNIP database (IAEA and WMO, 2017)); (b) tritium concentrations in North America in June 1963 (monthly mean); (c) permafrost classification across Canada (from NASA Earth Observatory Program (2016)); and (d) the change in mean annual air temperature in Canada from 1948 to 2012 (from the Government of Canada (2015)). Sample locations included in this study are shown as green points and HTO values are expressed as Tritium Units (T.U.). (For interpretation of the references to colour in this figure legend, the reader is referred to the Web version of this article.)

conductivity is low and waters typically have a long residence time within a watershed. In a region of discontinuous permafrost and peat plateaus in northern Alberta, Gibson et al. (2015) found that unfrozen wetlands contained tritium-enriched waters from 1960s precipitation, which were attributed to long water residence times in a low-hydraulic conductivity peat landscape.

Positioned between the active layer and the permafrost is an ice-rich and solute-rich layer called the transition zone (Shur et al., 2005; Kokelj and Burn, 2005). Using a stable isotope approach, Wang et al. (2018) found that active layer water sourced from precipitation was the dominant source of this ground ice near the permafrost table. The transition zone experiences freeze-thaw transitions on a sub-decadal to multi-centennial scale (Shur et al., 2005). The top of the transition zone is most susceptible to thaw when active layer thaw is deep enough to penetrate the zone (Shur et al., 2005). With deeper active layer thaw occurring in many permafrost regions due to rising mean annual air and ground temperatures, there is potential for these solutes, including tritium, to be released into surface waters. In regions with long water residence times, it could take many decades for this tritium-enriched water to leave the watershed and be dispersed (Gibson et al., 2015).

As described by Gibson et al. (2015), relatively old (i.e., pre-nuclear weapons test era) permafrost is expected to contain little or no tritium (i.e., < 10 T.U.), whereas modern permafrost that formed from post-

1950s precipitation is expected to contain significant tritium (i.e., > 10 TU.). Previous studies have shown that tritium is elevated in shallow permafrost that has formed since the 1950s as a result of moisture exchange between the active layer and permafrost (Michel and Fritz, 1978; Michel, 1986; Chizhov and Dereviagin, 1998). Burn and Michel (1988) show that tritium movement in permafrost is due to temperature-induced mass transport and not molecular diffusion, meaning that changes in ground temperature dynamics can result in tritium transport through permafrost.

1.3. Objectives and hypotheses

Only one study has assessed tritium concentrations in surface waters fed by melting permafrost. Gibson et al. (2015) recently conducted a study in northern Alberta in regions of isolated patches and sporadic discontinuous permafrost to better understand the linkage between permafrost thaw and water yield as part of a water budget assessment. The authors report that thaw lakes fed by melting permafrost were found to be significantly enriched in tritium compared to non-thaw lakes in the region, with tritium levels ranging from about 10.7 to 19.6 tritium units (T.U.; Gibson et al., 2015). The objective of this study was to assess tritium concentrations in lakes located along a gradient of sporadic, discontinuous and continuous permafrost zones experiencing degradation.

It was hypothesized that elevated tritium would be found in thaw lakes if they are fed by melting of modern (post-1950s) permafrost, particularly in lakes located in the discontinuous permafrost zone where permafrost degradation is most pronounced. Alternatively, lower tritium concentrations would be found in lakes sourced by melting of old (pre-1950s) permafrost, or lakes located in regions where permafrost is spatially continuous and has not yet experienced significant degradation. Further, it was hypothesized that in zones of permafrost degradation, tritium concentrations would be higher in groundwater seepage discharging to surface waters than in the receiving surface waters, due to less influence of dilution. Lastly, it was hypothesized that any permafrost melt-waters marked by elevated tritium would also be enriched with ions and dissolved organic carbon, scoured from peat and soils during sub-surface migration (as observed by Walvoord and Striegl (2007); Hickman (2016); Fouché et al. (2017); Roberts et al. (2017)), while they would be depleted in heavy stable isotopes of oxygen and hydrogen—showing a signature similar to frozen permafrost (Michel, 1986; Stotler et al., 2009). Results are discussed in the context of a better understanding of the fate and transport of tritium in the Arctic and sub-Arctic in light of a changing physical environment.

2. Material and methods

2.1. Study locations

A total of 23 water bodies (including lakes, ponds and wetlands—hereafter collectively referred to as ‘lakes’; see Table 1) were sampled over three broad regions varying in permafrost condition across northern Canada. Sampling was conducted in mid-September of 2016 (Northwest Territories and Labrador sites) and 2017 (northern Manitoba). These broad geographical regions are shown as green boxes in Fig. 1 and included (i) the Great Slave Lake region of the Northwest Territories (NT), (ii) the western Hudson Bay Lowlands region of Manitoba (MB) and (iii) the Wabush and Happy Valley–Goose Bay regions of Labrador (NL). Each of these three broad regions was broken into sub-regions based on geography, as shown in Fig. 1 and Table 1. From the Northwest Territories to Labrador, all study locations were characterized by similar landscape, hydrological and vegetation features. In particular, all sites are located within flat and low-lying extensive and poorly drained peatlands (palsa bog or fen), typically surrounded by black spruce (*Picea mariana*), white spruce (*Picea glauca*), jack pine (*Pinus banksiana*), balsam fir (*Abies balsamea*) and tamarack

(*Larix laricina*) forest overlying some degree of permafrost.

2.1.1. Great Slave plains

The Great Slave Lake region of the Northwest Territories lies within the Dry Continental Boreal ecoclimatic region within the Taiga Plains and Taiga Shield ecoregions. This was the most intensely sampled region in this study, as it straddles several permafrost zones and has experienced some of the largest temperature increases in Canada since the nuclear weapons test era (Fig. 1). Sample locations included two lakes northeast of Yellowknife (62°N, 114°W; extensive discontinuous permafrost), three lakes between Behchoko and Fort Providence within the Mackenzie Bison Sanctuary (61–62°N, 116°W; extensive discontinuous permafrost), three lakes near the community of Kakisa (61°N, 117°W; sporadic discontinuous permafrost) and three lakes near the community of Jean Marie River (61°N, 120°W; sporadic discontinuous permafrost; Fig. 2). Great Slave Lake, which spans both extensive discontinuous and sporadic discontinuous permafrost zones (Table 1; Fig. 2), was also sampled in the north arm near Edzo. The Great Slave Lake region is characterized by dramatic seasonal changes in air temperatures, with annual mean air temperature ranging from about –3 to –6 °C (January mean = –28 °C; July mean = 17 °C) and mean annual precipitation ranging from about 270 to 370 mm across the study region (Environment Canada, 2017, Table 1). Permafrost depth in this region ranges from ~60 m north of Yellowknife to 0–15 m in the southern and western parts (Brown, 1970; Judge, 1973). The Great Slave Lake region is currently experiencing some of the greatest rises in temperature anywhere in the world, with mean temperatures increasing between two and 3 °C from 1948 to 2012 (Fig. 1d) and changes in permafrost have been well documented in this region (e.g., Smith et al., 2009, Smith, 2011; Quinton et al., 2011; Bouchard et al., 2017).

2.1.2. Western Hudson Bay Lowlands

The Hudson Bay Lowlands is the world's second largest continuous wetland. The Churchill, Manitoba region (58°N, 94°W) lies within the High Subarctic ecoclimatic region within the Hudson Plains ecoregion along the southwestern shore of Hudson Bay and is marked by short, cool summers and long, very cold winters. Mean annual air temperature near Churchill is about –7 °C (January mean = –27 °C; July mean = 12 °C), mean annual ground temperature is about –1 to –2 °C and mean annual precipitation is about 417 mm (Smith et al., 2010; Environment Canada, 2017). The region has a very cold, humid subarctic climate and peatlands dominate the landscape. The flat terrain and continuous permafrost underlying this region impedes infiltration resulting in water pooling on the surface, which creates thousands of shallow lakes, ponds and wetlands—mainly of thermokarst origin (Bouchard et al., 2017). Permafrost thickness in the Churchill region is approximately 60–80 m (Brown, 1970; Dredge, 1992). Owing to poor drainage, trees are typically found at drier, higher altitudes and are absent at lower altitudes. A total of six lakes near Churchill, all located within the continuous permafrost zone, were sampled (Table 1; Fig. 1; Fig. 2). The Churchill River, approximately 19 km upstream from its discharge into Hudson Bay, and a groundwater monitoring well, located within an area of peat plateau, approximately 20 km east of Churchill, were also sampled.

2.1.3. Eastern Taiga Shield

The Wabush (53°N, 67°W) and Happy Valley–Goose Bay (53°N, 60°W) regions of Labrador lie within the Mid-Subarctic ecoclimatic region of the Taiga Shield. Two lakes near Wabush and two lakes near Happy Valley–Goose Bay were sampled, all located within isolated patches of permafrost (Fig. 1; Table 1; Fig. 2). A road-side gravity spring near Wabush was also sampled opportunistically. This region is characterized by cool summers and very cold winters. In the Wabush region, mean annual air temperature is about –3.8 °C (January mean = –22 °C; July mean = 13 °C) and mean annual precipitation is about 892 mm (Environment Canada, 2017). Permafrost is found in

Table 1
Physical and environmental characteristics of study water bodies.

Region	Location	MAAT (°C)	MAGT (°C)	MAP (mm)	Ecozone	Permafrost Zone [†]	Water Body ID	Common Name	Type of Water Body	Latitude	Longitude	Elev. (masl)
Labrador	Wabush	-3.8	0.9	892	Taiga Shield	Isolated Patches	WB-1	—	Wetland (fen)	53°04'04"	66°11'23"	560
Labrador	Wabush	-3.8	0.9	892	Taiga Shield	Isolated Patches	WB-2	De Mille Lake	Small lake	53°01'51"	66°34'21"	547
Labrador	Wabush	-3.8	0.9	892	Taiga Shield	Isolated Patches	WB-spring	—	Natural spring	53°03'57"	66°29'40"	663
Labrador	Happy Valley	-1.9	-0.7	946	Taiga Shield	Isolated Patches	HV-1	Wetland (bog)	Small lake	53°12'46"	60°25'16"	44
Labrador	Happy Valley	-1.9	-0.7	946	Taiga Shield	Isolated Patches	HV-2	Gosling Lake	Small lake	53°25'10"	60°22'38"	39
Manitoba	Churchill	-7.6	-1.6	417	Hudson Plains	Continuous	CH-1	Ramsay Lake	Small lake	58°33'20"	93°47'06"	17
Manitoba	Churchill	-7.6	-1.6	417	Hudson Plains	Continuous	CH-2	Lord Lake	Small lake	58°43'54"	93°53'49"	10
Manitoba	Churchill	-7.6	-1.6	417	Hudson Plains	Continuous	CH-3	West Twin Lake	Small lake	58°37'45"	93°49'44"	23
Manitoba	Churchill	-7.6	-1.6	417	Hudson Plains	Continuous	CH-4	Lake A	Small lake	58°45'48"	93°49'39"	5
Manitoba	Churchill	-7.6	-1.6	417	Hudson Plains	Continuous	CH-5	Churchill River	Large river	58°37'32"	94°15'52"	6
Manitoba	Churchill	-7.6	-1.6	417	Hudson Plains	Continuous	CH-6	Golf Lake	Small lake	58°45'01"	93°58'13"	14
Manitoba	Churchill	-7.6	-1.6	417	Hudson Plains	Continuous	CH-7	Landing Lake	Small lake	58°41'22"	94°03'10"	15
Manitoba	Churchill	-7.6	-1.6	417	Hudson Plains	Continuous	CH-well	Monitoring well	—	58°12'38"	93°50'27"	23
NWT	Yellowknife	-5.7	-1.2	280	Taiga Shield	Extensive Discontinuous	YK-1	Pontoon Lake	Small lake	62°54'21"	114°00'87"	181
NWT	Yellowknife	-5.7	-1.2	280	Taiga Shield	Extensive Discontinuous	YK-2	Prosperous Lake	Small lake	62°35'24"	114°11'54"	177
NWT	Behchoko	-5.4	-1.0	272	Taiga Plains	Extensive Discontinuous	BK-1	Caen Lake	Small lake	61°39'29"	116°58'16"	212
NWT	Behchoko	-5.4	-1.0	272	Taiga Plains	Extensive Discontinuous	BK-2	—	Small lake	61°53'49"	116°33'17"	229
NWT	Behchoko	-5.4	-1.0	272	Taiga Plains	Extensive Discontinuous	BK-3	Birch Lake	Small lake	62°03'51"	116°31'02"	198
NWT	Jean Marie River	-3.6	-0.9	369	Taiga Plains	Sporadic Discontinuous	JM-1	Ekai Lake	Small lake	61°17'27"	120°35'25"	248
NWT	Jean Marie River	-3.6	-0.9	369	Taiga Plains	Sporadic Discontinuous	JM-2	Sanguez Lake	Small lake	61°15'19"	120°29'39"	257
NWT	Jean Marie River	-3.6	-0.9	369	Taiga Plains	Sporadic Discontinuous	JM-3	Gargan Lake	Small lake	61°14'51"	120°22'48"	269
NWT	Kakisa	-3.3	-0.9	343	Taiga Plains	Sporadic Discontinuous	KS-1	Heart Lake	Small lake	60°50'06"	116°39'21"	254
NWT	Kakisa	-3.3	-0.9	343	Taiga Plains	Sporadic Discontinuous	KS-2	—	Small lake	61°00'35"	117°29'14"	248
NWT	Kakisa	-3.3	-0.9	343	Taiga Plains	Sporadic Discontinuous	KS-3	Foetus Lake	Small lake	60°58'45"	118°21'37"	307
NWT	Great Slave	—	—	Taiga Shield/Plains	-various zones-	GSL	Great Slave Lake	Large lake	62°58'24"	113°94'26"	156	

Notes: Labrador and Northwest Territories (NWT) sites sampled in September 2016, Manitoba sites samples in September 2017; MAAT = mean annual ground temperature; MAGT = mean annual air temperature; MAP = mean annual precipitation; see Fig. 2 for a map of these sites. [†] % of land underlain by permafrost in isolated patches (0–10%), sporadic discontinuous (10–50%), extensive discontinuous (50–90%) and continuous (90–100%), as defined by Brown et al. (2001) and NASA (2017).

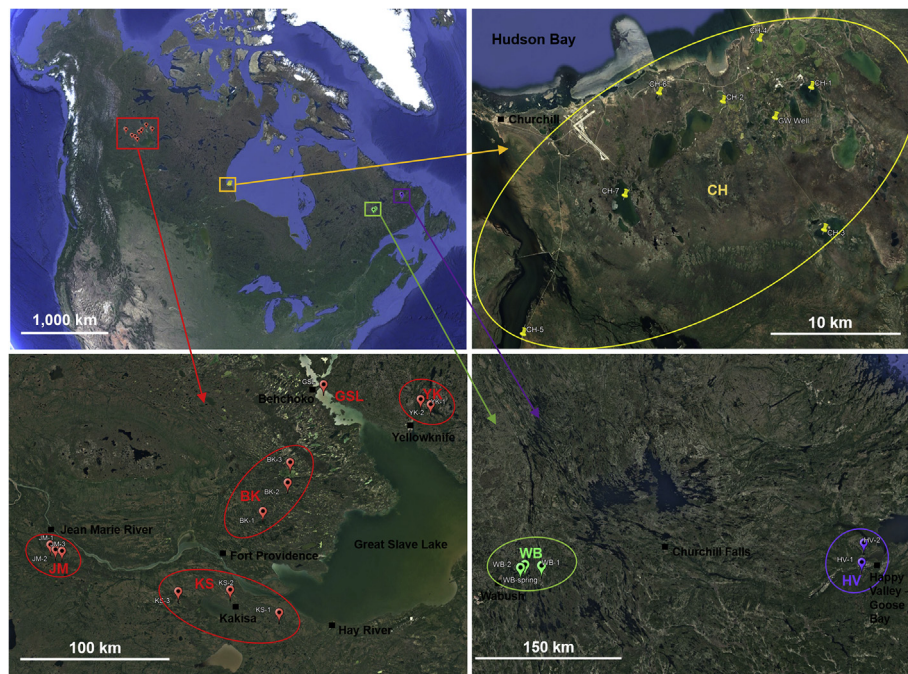


Fig. 2. Locations of sample sites across northern Canada (top left), showing the Great Slave Lake basin in the Northwest Territories (bottom left, red), the Churchill region of Manitoba (top right, yellow), and the Wabush (green) and Happy Valley (purple) regions of Labrador (bottom right). Sample lake groupings are identified by ellipses and are based on geography and extent of underlying permafrost (note differences in scale among regions). Imagery provided by Google Earth Pro (version 7.3.1.4507, Google, Inc., Mountain View, CA, USA). (For interpretation of the references to colour in this figure legend, the reader is referred to the Web version of this article.)

isolated patches with relatively low ice content (Brown, 1970). Deep, well drained glacial deposits cover much of the region, and wetland coverage is minimal (~1%; Riley et al., 2013). The Happy Valley–Goose Bay area is on the Labrador coast and is warmer (MAT of -1.9°C ; (January mean = -17°C ; July mean = 16°C) and wetter (MAP of 946 mm) than Wabush on the interior (Riley et al., 2013). Permafrost occurs in isolated patches, occurring only in peatlands (Brown et al., 2001). Wetlands cover about 9% of the region's land area (Riley et al., 2013). The spatial coverage of discontinuous and sporadic permafrost in Labrador has been disputed in the literature, and different coverage maps have been presented by Brown (1970), Payette and Rochefort (2001) and Way and Lewkowicz (2016).

2.2. Sample collection and preparation

At each study lake, five replicate surface water samples were collected. Surface water samples were collected using a peristaltic pump and were filtered in the field using a $0.2\text{ }\mu\text{m}$ Whatman Polydisc in-line filter. In addition, another five replicate groundwater seepage samples were collected from each water body. Locations of groundwater discharge along the shoreline were identified using thermal imaging, as the difference in temperature between groundwater and surface water can be used to delineate groundwater discharge zones (Banks et al., 1996). At each sample location, a shoreline survey was conducted using a Forward Looking Infrared Radiometer (FLIR, model T450sc) thermal imaging camera to locate zones of groundwater seepage (cold groundwater seepage discharging to relatively warmer surface water). Sample collection was conducted in September when surface waters are near their warmest, so locations of cool groundwater seepage could be identified using thermal imaging.

Once shoreline seepage zones were identified, mini-piezometers were installed following methods from Lee and Cherry (1979). Piezometers were typically pounded 1.25–1.50 m into the bottom substrate (until refusal), and were left for 24 h to passively collect groundwater seepage samples in a collection bag. The following day, samples were filtered using a $0.2\text{ }\mu\text{m}$ Whatman Polydisc in-line filter and a peristaltic pump and transferred from the collection bag into polyethylene scintillation vials. After collection, water samples were vacuum sealed inside a bag and placed on dry ice in a dark cooler where they were transported to the low-background laboratory and kept frozen in the

dark until analysis.

2.3. Sample analysis

2.3.1. General water chemistry measurement

Electrical conductivity ($\mu\text{S}\cdot\text{cm}^{-1}$) and pH measurements were taken at room temperature for all water samples using a benchtop multi-parameter meter (Orion Star A215, ThermoScientific, USA). Analysis of major ions was conducted using an Ion Chromatography System (ICS; Dionex ICS 1100, ThermoScientific, USA). The ICS was calibrated with National Institute of Standards and Technology (NIST) traceable multi-anion/cation certified standards. For the determination of dissolved organic carbon (DOC), samples were analyzed on a Teledyne-Tekmar Fusion analyzer, using the UV persulfate oxidation method of determining the carbon content within the sample. Calibration curves were established using certified organic and inorganic standards (1000 ppm C, Ricca Chemical Co., Arlington, TX, USA) prior to sample analysis.

2.3.2. Stable isotope measurement

Water samples were analyzed for stable oxygen and hydrogen isotopes for determination of $\delta^{18}\text{O}$ and $\delta^2\text{H}$, which can help to identify the origin of water samples (Clark and Fritz, 1997). Hydrogen and oxygen isotope composition was determined at the University of Ottawa's G.G. Hatch Stable Isotope Laboratory using a Finnigan MAT DELTAplus XP and Gasbench (Thermo-Fisher Scientific) following methods from deGroot (2004). Samples were analyzed for hydrogen and oxygen separately. A precise amount (0.2 mL) of water was pipetted into Exetainer vials and a platinum catalyst pellet on a stick was added to each Exetainer for H analysis (no catalyst was added for O analysis). The vials were flushed and filled with a gas mixture (2% H_2 for H samples, 2% CO_2 for O samples) in helium off-line, and the flushed vials were left at room temperature for 24 h. The H_2 and CO_2 gasses were then analyzed automatically in continuous flow. The precision (2 sigma) of the analysis was ± -2.0 per mil (‰) for hydrogen isotopes and $\pm -0.15\text{‰}$ for oxygen isotopes. All results were normalized to Vienna Standard Mean Ocean Water (VSMOW) using three calibrated internal standards spanning most of the natural range.

2.3.3. Tritium measurement

Tritium analysis of all surface water and groundwater seepage samples was conducted at the low-background environmental laboratory at Chalk River Laboratories. For each of the triplicate samples, 10 mL of water was mixed with 10 mL of UltimaGold LLT (PerkinElmer, USA) in a 20 mL polyethylene low-static liquid scintillation vial (Packard, USA) and tritiated water (HTO) activity concentrations (Bq L^{-1}) were determined directly using a low-activity liquid scintillation counter (LSC; PerkinElmer Quantulus GCT 6220) with three count cycles and a 120 min count time for each cycle. The minimum detectable activity (MDA) for the 10 mL water samples ranged from 1.29 to 1.74 Bq L^{-1} and the typical background was about 0.8 Bq L^{-1} in the LSC during these measurements. All analytical runs in the LSC included duplicate method blanks (tritium-free dead water, $\leq 0.1 \text{ Bq L}^{-1}$), a low-activity standard (NIST, $\sim 9.8 \text{ Bq L}^{-1}$), a high-activity standard (NIST, $\sim 96.4 \text{ Bq L}^{-1}$) and a spike ($\sim 16,000 \text{ Bq L}^{-1}$). In all cases, the method blanks were less than the detection limit and the standards and spikes were within 7% and 6% of expected values, respectively. Tritium concentrations are presented in both Bq L^{-1} and tritium units (T.U.), with one T.U. equal to one ${}^3\text{H}$ per 10^{18} H atoms (or, 1 T.U. = 0.1181 Bq L^{-1} ; Kazemi et al., 2006).

2.4. Data analysis

For each water body, the tritium results for the triplicate samples were combined to produce a mean value (\pm standard error). Statistical comparisons of tritium concentrations were considered both at the lake grouping scale shown in Fig. 2, and by re-grouping the lakes according to the extent of permafrost underlying the local landscape (as shown in Fig. 1c). A Kruskal-Wallis one-way Analysis of Variance (ANOVA) on Ranks was used to compare tritium concentrations among sample groups, as data did not satisfy the assumptions of normal distribution or equal variances. If a statistical difference was detected, Dunn's *post-hoc* test was used for pairwise multiple comparisons among groups (Quinn and Keough, 2002). Historical tritium concentration data for a number of locations around Canada was obtained from the International Atomic Energy Agency's (IAEA) Water Resources Programme for precipitation and river water (IAEA and WMO, 2017). Tritium values were also extracted from the literature for comparison with the results of this study, and were typically measured in permafrost cores, frozen peat, glacial ice cores, Arctic lakes and sub-permafrost groundwaters (e.g., Koerner and Taniguchi, 1976; Jeffries et al., 1984; Michel, 1986; Burn and Michel, 1988; Chizhov and Dereviagin, 1998; Kotzer et al., 2000; Blais et al., 2001; Clark et al., 2007; Calmels et al., 2008; Wu et al., 2010; Van der Wel et al., 2011; Kang et al., 2015). All tritium concentrations discussed in this paper, both measured and extracted from the literature, have been decay-corrected to November 2017 using a $t_{1/2}$ of 12.32 years so that activity concentrations can be standardized and compared.

Patterns of correlation between environmental variables were identified using a Pearson correlation matrix with Bonferroni-adjusted significance values to control for Type I error (Quinn and Keough, 2002). To assess the similarity of the paired (surface water and groundwater) geochemical measures at study lake, the Wilcoxon Signed-rank test was used. Principal components analysis (PCA) was used to summarize the major patterns of variation within the data and to ordinate the sample sites with respect to their physical, chemical, radiochemical and limnological characteristics (Quinn and Keough, 2002). The PCA included a mix of continuous and categorical data. Continuous data included pH, EC, DOC, Fl^- , PO_4^{3-} , NO_3^- , NH_4^+ , SO_4^{2-} , Mg^{2+} , Ca^{2+} , K^+ , Na^+ , Cl^- , ${}^2\text{H}$, ${}^{18}\text{O}$, HTO, MAP, MAGT, MAAT, ELEV, LONG and LAT (see Tables 1 and 2 for data). Ecozone (Taiga Shield [TAIG-SH], Taiga Plains [TAIG-PL] or Hudson Plains [HUDS-PL]), underlying permafrost extent (isolated patches [PERM-IP], sporadic discontinuous [PERM-SD], extensive discontinuous [PERM-ED] or continuous [PERM-C]; according to Brown et al. (2001); Smith and Burgess (2004); NASA (2017)) were included as binary codes

(0 = false or 1 = true) in the PCA. Permafrost sensitivity to thaw (THAW SENS) was coded by region as a 1 (low), 2 (medium) or 3 (high), according to Smith and Burgess (2004). The change in mean annual air temperature since 1948 (Δ TEMP; see Fig. 1d) was extracted from a climate change report by the Government of Canada (2015). A number of variables, including NO_2^- , N^- , Br^- and Li^+ , were excluded from the PCA because their concentrations were frequently at or below the analytical detection limit. All data analysis was conducted using either SigmaPlot (version 12.5, Systat Software, Inc., San Jose, CA, USA), or PAST (version 3.17, Hammer et al., 2001) software packages, using a significance level of 0.05.

3. Results

3.1. Tritium

Tritium concentrations are highly variable among sample locations, ranging from less than the detection limit ($< \sim 12 \text{ T.U.}$) in northern Manitoba to about 128 T.U. in parts of the Northwest Territories (Table 2; Fig. 3). Tritium concentrations in groundwater discharging to water bodies were not higher than ambient surface water concentrations (paired $t = 0.144$, $p = 0.887$, $n = 23$). As shown in Fig. 4, this data was highly variable, with some water bodies having higher tritium concentration in groundwater discharge than in ambient surface water (e.g., KS-1, BK-1, BK-2, JM-2, YK-2), while other water bodies had higher tritium concentration in surface water than in groundwater discharge (e.g., JM-1, JM-3, KS-2, YK-1). The highest observed tritium concentrations are from Ekali Lake (JM-1; 128 T.U.), Sanguez Lake (JM-2; 92 T.U.) and Gargan Lake (JM-3; 92 T.U.), all located near Jean Marie River, Northwest Territories along the transition zone from sporadic discontinuous to extensive discontinuous permafrost (Table 2).

Among permafrost zones, the mean tritium values for surface waters were found to be $\sim 11.49 \pm 0.52 \text{ T.U.}$ in lakes located in the continuous permafrost zone (near Churchill, MB), $53.47 \pm 7.03 \text{ T.U.}$ in lakes located in the extensive discontinuous permafrost zone (Behchoko and Yellowknife, NT), $63.76 \pm 15.34 \text{ T.U.}$ in lakes located in the sporadic discontinuous permafrost zone (Jean Marie River and Kakisa, NT), and $16.43 \pm 1.71 \text{ T.U.}$ in lakes located in the isolated patches permafrost zone (Wabush and Happy Valley-Goose Bay, NL). Differences among these groups were statistically significant (K-W ANOVA, $H_3 = 16.77$, $p < 0.001$), with tritium values for sporadic discontinuous and extensive discontinuous permafrost zones greater than those for the continuous and isolated patches permafrost zones ($p < 0.05$; Fig. 3). Likewise, groundwater seep tritium content varied significantly among sample locations (K-W ANOVA, $H_3 = 18.11$, $p < 0.001$), with concentrations of $11.32 \pm 0.48 \text{ T.U.}$ in groundwater located in the continuous permafrost zone, $61.16 \pm 6.67 \text{ T.U.}$ in the extensive discontinuous permafrost zone, $51.82 \pm 9.20 \text{ T.U.}$ in the sporadic discontinuous permafrost zone and $21.37 \pm 4.39 \text{ T.U.}$ in groundwaters located in the isolated patches permafrost zone (Fig. 3).

Data were compared to decay-corrected reference values for tritium, including (i) weapons-test era (1961–1967) precipitation for Fort Smith, Whitehorse, Ottawa and Happy Valley-Goose Bay; (ii) recent precipitation from Ottawa (2005–12); (iii) present day concentrations in Ottawa River water; (iv) permafrost and ice core data from the literature (Koerner and Taniguchi, 1976; Jeffries et al., 1984; Michel, 1986; Burn and Michel, 1988; Chizhov and Dereviagin, 1998; Kotzer et al., 2000; Van der Wel et al., 2011; Calmels et al., 2008; Kang et al., 2015); and (v) permafrost-thaw lakes in northern Alberta studied by Gibson et al. (2015). Box plots of the enriched tritium concentration in the permafrost-thaw fed lakes, other waterbodies, and a variety of reference samples are shown in Fig. 3 using the tritium data provided in Table 2.

The enriched tritium concentrations observed in surface waters and groundwaters near the Northwest Territories communities of Jean Marie River and Kakisa (underlain by sporadic discontinuous

Table 2

Water geochemistry data for groundwater and surface water samples included in this study, including pH, electrical conductivity (EC), dissolved organic carbon (DOC), major anions and cations, stable oxygen and hydrogen isotopes and tritium. Tritium values represent the mean \pm standard error of triplicate samples (presented in both Bq L^{-1} and tritium units [T.U.]), while all other water chemistry measures are based on a single sample per sample ID.

Sample ID	pH	EC $\mu\text{S/cm}$	DOC mg/L	Major Anions mg/L				Major Cations mg/L				Stable Isotopes %				Tritium (HTO mean \pm SE)									
				Fl ⁻	Cl ⁻	NO ₂ ⁻	Br ⁻	NO ₃ ⁻	N	PO ₄ ³⁻	SO ₄ ²⁻	Li ⁺	Na ⁺	NH ₄ ⁺	K ⁺	Mg ²⁺	Ca ²⁺	⁸ He	⁸ He	Bq/L	\pm SE	T.U.	\pm SE		
Wabush, NL; 53°N latitude; Isolated Patches of permafrost																									
WB-1-SW	6.00	18	6.9	0.02	2.03	< 0.08	0.03	< 0.01	0.49	0.29	< 0.01	1.6	0.05	1.70	0.47	2.6	-14.3	-106.1	1.97	0.09	16.68	0.75			
WB-1-GW	6.54	52	15.5	0.02	5.60	< 0.08	0.13	0.03	0.64	0.64	< 0.01	3.0	2.51	2.61	0.50	11.8	-14.7	-108.3	1.90	0.36	16.09	3.03			
WB-2-SW	6.26	43	3.6	0.04	1.51	< 0.08	< 0.02	< 0.01	0.41	1.87	< 0.01	1.3	< 0.02	2.20	2.51	7.50	-14.1	-105.1	2.30	0.26	19.48	2.18			
WB-2-GW	5.92	31	4.0	0.05	1.94	< 0.08	< 0.02	< 0.01	0.55	0.42	< 0.01	2.4	0.45	2.92	1.00	5.21	-14.1	-102.0	2.50	0.16	21.17	1.34			
WB-spring	6.68	26	3.3	0.03	0.62	< 0.08	< 0.02	0.03	< 0.19	1.60	< 0.01	1.6	< 0.02	0.70	1.83	6.62	-15.8	-112.4	4.11	0.63	34.80	5.27			
Happy Valley–Goose Bay, NL; 53°N latitude; Isolated Patches of permafrost																					< 1.38	–	< 11.69	–	
HV-1-SW	4.96	16	6.9	0.04	3.13	< 0.08	< 0.02	0.03	< 0.01	0.63	< 0.22	< 0.01	1.1	0.12	1.53	0.17	0.25	-8.6	-74.5	< 1.44	–	< 12.19	–		
HV-1-GW	4.79	19	11.1	0.03	3.00	< 0.08	< 0.02	0.03	< 0.01	0.52	< 0.22	< 0.01	1.0	0.58	1.30	0.12	0.47	-12.8	-97.5	2.17	0.45	18.37	3.78		
HV-2-SW	6.39	88	7.9	0.06	70.0	< 0.08	0.14	< 0.02	< 0.01	0.21	5.89	< 0.01	26.0	0.03	8.88	3.10	2.60	-14.1	-105.9	2.50	0.16	21.17	1.34		
HV-2-GW	6.92	404	6.1	< 0.01	258	< 0.08	0.73	0.32	0.07	0.23	6.93	< 0.01	127	0.39	7.40	13.5	7.10	-14.6	-108.3	3.16	0.75	26.76	6.32		
Behchoko, NT; 61 to 62°N latitude; Extensive Discontinuous permafrost																					4.43	2.18	37.51	18.45	
BK-1-SW	8.21	427	9.8	0.16	2.74	< 0.08	< 0.02	< 0.02	< 0.01	0.19	542	< 0.01	16.4	0.78	5.47	43.3	117.4	-8.7	-101.0	67.4	82.8	-8.6	-99.3	8.09	
BK-1-GW	8.32	450	14.2	0.29	5.54	< 0.08	0.06	0.04	< 0.01	0.19	560	0.03	26.7	1.22	9.11	67.4	82.8	-8.6	-98.8	4.82	4.82	40.81	6.85		
BK-2-SW	7.94	107	12.2	0.09	2.59	< 0.08	< 0.02	< 0.02	< 0.01	0.19	73	< 0.01	4.7	< 0.02	2.56	12.6	34.8	34.9	112.3	9.1	9.1	12.6	7.98		
BK-2-GW	7.92	127	18.4	0.32	6.29	< 0.08	< 0.02	< 0.02	< 0.01	0.19	252	< 0.01	12.0	0.40	< 0.02	1.64	7.63	53.7	-9.8	-106.5	6.87	6.87	58.17	3.45	
BK-3-SW	8.14	128	13.7	0.14	3.64	< 0.08	< 0.02	< 0.02	< 0.01	0.19	94	< 0.01	4.0	< 0.02	0.02	1.77	45.6	119.7	-9.3	-101.6	5.52	5.52	46.74	20.81	
BK-3-GW	8.16	458	19.3	0.29	18.91	< 0.08	< 0.02	0.93	2.24	< 0.19	365	0.02	21.8	1.17	9.77	5.46	2.33	1.42	2.33	5.46	26.9	-11.3	-110.3	8.28	
Yellowknife, NT; 62°N latitude; Extensive Discontinuous permafrost																					-126.1	9.09	2.83	76.97	23.78
YK-1-SW	8.52	291	16.3	0.04	1.89	< 0.08	< 0.02	< 0.02	< 0.01	0.19	2.9	< 0.01	1.3	< 0.02	0.48	0.76	10.9	-14.0	-127.1	5.28	0.94	44.71	7.92		
YK-2-SW	7.36	35	5.6	0.28	8.29	< 0.08	0.05	< 0.02	< 0.01	0.19	1.2	< 0.01	0.83	< 0.02	0.07	9.11	16.5	-13.6	-122.7	6.41	0.49	54.27	4.14		
YK-2-GW	7.25	244	8.9	0.18	4.03	< 0.08	0.04	0.01	< 0.01	0.19	0.3	< 0.01	0.32	< 0.01	0.2	1.42	2.33	5.46	2.33	10.90	3.77	92.29	31.71		
Great Slave Lake, NT; 60 to 62°N latitude; Spans both Extensive Discontinuous & Sporadic Discontinuous permafrost																					10.87	0.06	92.04	0.47	5.82
GSL-SW	7.81	34	6.1	0.04	2.53	< 0.08	< 0.02	< 0.02	< 0.01	0.19	35	< 0.01	7.0	< 0.02	0.66	6.15	24.4	-9.6	-102.3	3.38	0.82	28.62	6.97		
GSL-GW	7.77	53	7.2	0.05	42.6	< 0.08	0.11	0.03	< 0.19	0.5	< 0.01	19.6	< 0.02	1.20	3.22	11.3	-10.9	-109.0	3.63	1.57	30.74	13.27			
Jean Marie River, NT; 61 to 62°N latitude; Sporadic Discontinuous permafrost																					5.31	20.9	-16.8	15.16	16.82
JM-1-SW	7.97	60	16.1	0.03	3.20	< 0.08	< 0.02	< 0.02	< 0.01	0.19	12.6	< 0.01	4.3	< 0.02	1.29	5.31	20.9	-16.8	-142.4	1.31	1.31	42.76	13.26		
JM-1-GW	7.93	45	22.3	0.04	0.68	< 0.08	< 0.02	< 0.02	< 0.01	0.19	3.0	0.01	1.0	< 0.02	0.28	1.31	14.9	-16.7	-141.4	5.05	5.05	1.58	44.71	11.40	
JM-2-SW	7.89	72	15.1	0.22	0.73	< 0.08	< 0.02	0.04	< 0.01	0.19	29.0	< 0.01	2.5	0.10	1.44	10.20	14.0	-13.6	-125.6	5.28	1.36	44.71	11.40		
JM-2-GW	7.85	94	19.9	0.25	0.54	< 0.08	< 0.02	4.60	1.04	< 0.19	101	< 0.01	3.0	< 0.02	1.93	18.80	40.5	-13.5	-126.9	10.90	10.90	3.77	92.29	31.71	
JM-3-SW	7.93	90	16.9	0.02	1.39	< 0.08	< 0.02	< 0.02	< 0.01	0.19	0.9	< 0.01	1.1	< 0.02	0.30	1.18	5.60	-16.7	-138.0	10.87	0.06	92.04	0.47		
JM-3-GW	7.91	166	24.8	0.02	8.73	< 0.08	0.16	8.07	1.82	< 0.19	0.9	< 0.01	2.2	< 0.02	0.99	28.8	47.6	-18.6	-153.2	6.97	6.97	59.02	5.82		
Kakisa, NT; 60 to 61°N latitude; Sporadic Discontinuous permafrost																				5.53	28.0	-16.3	-134.8	4.36	
KS-1-SW	7.81	48	14.6	0.04	0.51	< 0.08	< 0.02	< 0.02	< 0.01	0.97	0.22	< 0.01	1.0	< 0.01	1.5	0.29	0.45	4.18	36.8	-14.0	-127.6	4.11	0.61	34.80	5.09
KS-1-GW	7.88	110	19.5	0.04	0.89	< 0.08	< 0.02	< 0.02	< 0.01	0.19	3.2	< 0.01	12.0	0.06	0.62	9.13	19.1	-10.9	-88.4	< 1.29	< 1.29	< 10.92	–		
KS-2-SW	7.18	282	6.9	0.07	68.0	< 0.08	0.17	0.19	0.44	0.44	< 0.01	3.0	2.51	< 0.01	2.32	2.10	21.2	60.3	12.1	6.44	1.72	54.53	14.44		
KS-2-GW	7.67	330	9.1	0.16	169.0	< 0.08	0.25	< 0.02	< 0.01	0.19	5.89	< 0.01	26.0	0.03	7.50	25.3	28.0	-9.8	-88.0	< 1.29	< 1.29	< 10.92	–		
KS-2-GW	7.54	667	12.2	< 0.01	312.3	< 0.08	0.59	< 0.02	< 0.01	0.19	0.49	< 0.01	136.1	2.70	12.0	41.1	101.3	-12.7	-101.8	< 1.34	< 1.34	< 11.35	–		
CH-3-SW	8.02	76	4.3	0.10	8.83	< 0.08	0.02	< 0.02	< 0.01	0.19	0.09	< 0.01	4.4	< 0.02	< 0.05	5.72	17.4	-9.5	-84.6	< 1.42	< 1.42	< 12.02	–		
CH-3-GW	7.95	221	3.6	0.42	15.0	< 0.08	0.33	0.22	0.96	0.22	< 0.01	6.1	< 0.01	6.4	< 0.02	4.11	19.4	64.5	-15.5	-116.3	5.94	5.94	70.30	6.40	
CH-4-SW	7.64	319	12.2	< 0.01	141.0	< 0.08	0.33	< 0.02	< 0.01	0.19	34.0	< 0.01	77.1	< 0.02	6.60	21.0	28.0	-9.8	-86.2	< 1.43	< 1.43	< 12.11	–		
CH-4-GW	7.78	5421	5.8	< 0.01	9.435	< 0.08	20.0	19.1	4.33	< 0.19	97.0	< 0.01	31.30	< 0.02	84.0	25.9	152	-10.3	-88.2	< 1.45	< 1.45	< 12.28	–		
CH-5-SW	7.81	319	8.4	0.05	141.0	< 0.08	0.31	< 0.02	< 0.01	0.19	13.2	< 0.01	50.0	< 0.											

Table 2 (continued)

Sample ID	pH	EC $\mu\text{s}/\text{cm}$	DOC mg/L	Major Anions mg/L								Major Cations mg/L								Stable Isotopes %			
				Fl ⁻	Cl ⁻	NO ₂ ⁻	Br ⁻	NO ₃ ⁻	N	PO ₄ ⁻	SO ₄ ⁻	Li ⁺	Na ⁺	NH ₄ ⁺	K ⁺	Mg ²⁺	Ca ²⁺	⁸² H	⁸¹ O	Bq/L	\pm SE	T.U.	\pm SE
CH-5-GW	7.92	5190	3.9	< 0.01	6168	< 0.08	16.0	< 0.02	< 0.01	< 0.19	482.2	< 0.01	2044	< 0.02	32.0	144	271.3	-13.5	-103.8	< 1.46	-	< 12.36	-
CH-6-SW	7.33	382	11.8	0.14	282.1	< 0.08	0.48	< 0.01	< 0.01	< 0.19	19.2	< 0.01	77.3	< 0.02	3.01	22.2	53.4	-10.4	-88.4	< 1.45	-	< 12.28	-
CH-6-GW	7.25	399	8.0	< 0.01	281.3	< 0.08	0.52	0.10	0.02	< 0.19	19.4	< 0.01	77.2	< 0.02	3.08	23.4	53.0	-10.4	-88.1	< 1.44	-	< 12.19	-
CH-7-SW	7.37	94	6.1	< 0.01	19.0	< 0.08	< 0.02	< 0.02	< 0.01	< 0.19	0.70	< 0.01	8.0	0.05	0.60	6.90	19.3	-10.4	-91.9	< 1.41	-	< 11.94	-
CH-7-GW	7.24	257	25.5	0.44	23.0	< 0.08	0.13	< 0.02	< 0.01	< 0.19	2.50	< 0.01	11.0	1.33	2.10	23.4	130.1	-13.8	-98.6	< 1.46	-	< 12.36	-
CH-well	7.86	98	35.6	< 0.01	19.3	< 0.08	0.44	< 0.02	< 0.01	< 0.19	9.02	< 0.01	16.1	< 0.02	0.10	8.04	21.0	-13.9	-99.3	< 1.39	-	< 11.77	-

Note: Reasons for the high EC values in samples CH-4-GW and CH-5-GW, caused by elevated Cl⁻ and Na⁺ concentrations, are unclear. However, CH-4-GW may be high due to close proximity to Hudson Bay (marine aerosols, Henkemans et al., 2018) and CH-5-GW may be high due to this sample site being located at the end of a road where road-salt-laden snow might be piled in the winter, potentially causing a localized NaCl plume. These EC, Na⁺ and Cl⁻ results were excluded from the correlation analyses presented in Table 3. Corresponding surface water samples from these sample locations are not elevated in EC.

permafrost) and Yellowknife and Behchoko (underlain by extensive discontinuous permafrost) are significantly higher than recent (2005–12) Ottawa precipitation (Mann-Whitney $U = 0.00$, $n_1 = 22$, $n_2 = 87$, $p < 0.001$), whereas there is no statistical difference in tritium between the enriched concentrations observed in Northwest Territories lakes in this study and the decay-corrected concentrations of weapons-era precipitation from nearby Fort Smith or Whitehorse ($U = 763$, $n_1 = 22$, $n_2 = 81$, $p = 0.305$), as shown in Fig. 3. Likewise, there is no significant difference in tritium content between present-day concentrations in the Northwest Territories thaw lakes and weapons-era tritium peak values extracted from the permafrost and ice core literature ($U = 85$, $n_1 = 9$, $n_2 = 22$, $p = 0.557$).

Tritium concentrations in all of the Churchill-area lakes, underlain by continuous permafrost, were below the detection limit ($< \sim 12$ T.U.) and likely reflect concentrations in recent precipitation (IAEA and WMO, 2017). Labrador samples, taken from waters underlain by isolated patches of permafrost, were also relatively low but showed more variability than those from Churchill. Groundwater seepage samples from Wabush (24.01 ± 3.25 T.U.) and Happy Valley–Goose Bay (17.82 ± 3.98 T.U.) were slightly elevated compared to the receiving surface waters (18.01 ± 1.48 T.U. and 15.03 ± 2.87 T.U., respectively). Present-day tritium concentrations in Labrador surface water and groundwater samples were compared with decay-corrected 1961–1967 precipitation data for nearby Happy Valley–Goose Bay and the present-day tritium content in the study lakes is significantly lower than decay-corrected weapons test-era precipitation ($U = 196$, $n_1 = 9$, $n_2 = 81$, $p = 0.024$), implying that these waters have been subject to significant hydrodynamic dispersion. Of particular note, water samples collected from a gravity spring near Wabush were slightly enriched in tritium (34.77 ± 5.33 T.U.), as shown in Fig. 5, but this water is significantly lower than decay-corrected 1961–1967 Happy Valley–Goose Bay precipitation based on a one-sample *t*-test ($t_{81} = 3.32$, $p = 0.001$), suggesting that this spring water contains a greater proportion of 1960s and 1970s precipitation than other surface waters in the region, but it has also undergone significant dilution and dispersion.

3.2. General water chemistry

As shown in Table 2, water chemistry varied greatly, both within and among study regions. When groundwater seepage samples and surface water samples were compared using the Wilcoxon Signed-rank test, it was found that groundwaters were typically enriched in ions associated with weathering processes, including chloride, potassium, sodium, magnesium, calcium, compared to the receiving surface waters ($[\text{Cl}^-]$, $W = 201$, $Z = 2.97$, $p = 0.003$, $r = 16$], $[\text{K}^+]$, $W = 235$, $Z = 2.95$, $p = 0.003$, $r = 19$], $[\text{Na}^+]$, $W = 228$, $Z = 2.30$, $p < 0.001$, $r = 18$], $[\text{Mg}^{2+}]$, $W = 238$, $Z = 3.04$, $p = 0.002$, $r = 17$] and $[\text{Ca}^{2+}]$, $W = 223$, $Z = 2.59$, $p = 0.009$, $r = 16$]). Consequently, ground waters were significantly higher in electrical conductance (EC) than receiving surface waters ($W = 224$, $Z = 3.77$, $p < 0.0001$, $r = 19$). Likewise, DOC was significantly higher in ground water seepage samples than in receiving surface waters ($t = -3.14$, $p = 0.005$, $n = 23$). Interestingly, this was overwhelmingly true for all lakes sampled in the Northwest Territories, but this was not the case for Churchill lakes where DOC was typically higher in surface waters than in groundwaters (Table 2). There was no difference in pH between surface and ground water samples (paired $t = -0.47$, $p = 0.641$, $n = 23$). As shown in Table 3, tritium activity concentrations are correlated with a number of environmental variables including water pH ($r = 0.421$, $p = 0.003$), DOC concentration ($r = 0.494$, $p < 0.001$), $\delta^2\text{H}$ ($r = -0.629$, $p < 0.001$), mean annual precipitation ($r = -0.394$, $p = 0.006$), mean annual temperature ($r = 0.357$, $p = 0.013$) and latitude ($r = 0.557$, $p < 0.001$). Stable isotopic composition ($\delta^2\text{H}$, $\delta^{18}\text{O}$) of groundwater seepage and surface water samples are presented in Table 2 and Fig. 7.

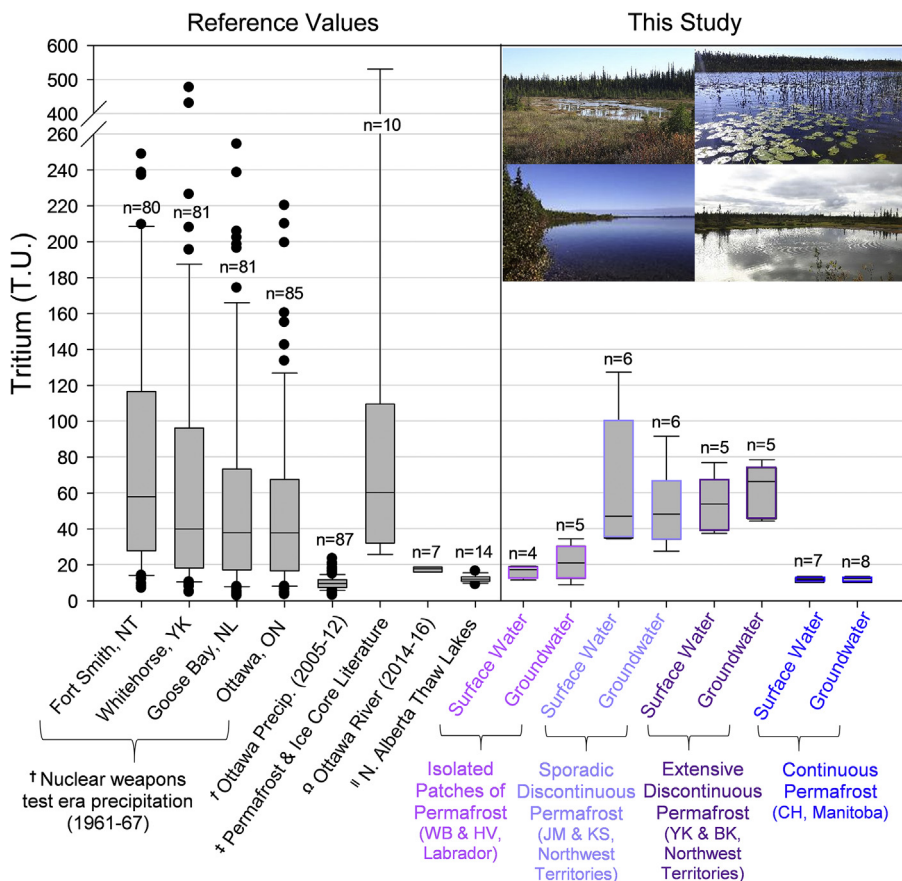


Fig. 3. Box plot showing tritium values in ground and surface-water samples in study lakes across a gradient of permafrost condition (right), compared to relevant reference values for tritium in the environment (left). All tritium values presented are decay-corrected to a common date (November 2017). Note the break in the y-axis between 260 and 400 T.U. Data sources for the reference values include (IAEA and WMO, 2017[†]), (Koerner and Taniguchi, 1976; Jeffries et al., 1984; Michel, 1986; Burn and Michel, 1988; Chizhov and Dereviagin, 1998; Kotzer et al., 2000; Van der Wel et al., 2011; Calmels et al., 2008; Kang et al., 2015[‡]), (CNL, 2017[§]) and (Gibson et al., 2015^{||}).

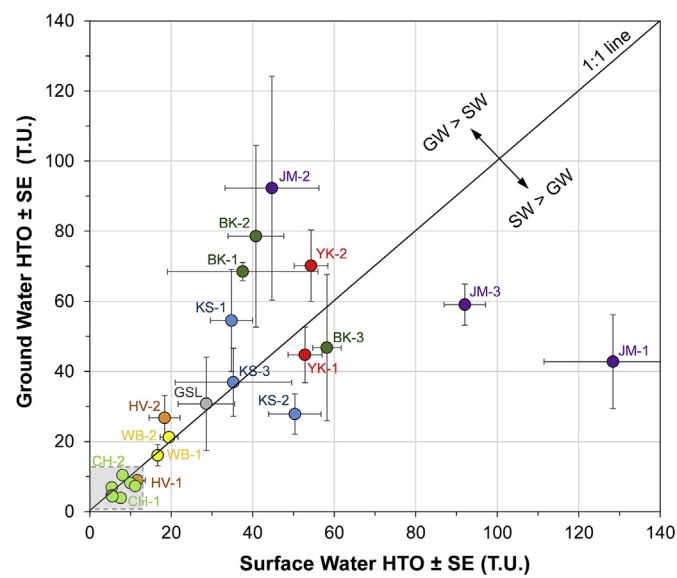


Fig. 4. Tritium concentrations in surface waters and ground waters for study lakes. Samples with tritium values < the detection limit (~12 T.U.) are shown in the greyed out area near the axis origins. Water bodies appearing above the 1:1 line have greater tritium in ground water discharge than in ambient surface water, while the opposite is the case for water bodies appearing below the 1:1 line. Water body IDs correspond with water body names and characteristics presented in Table 1.

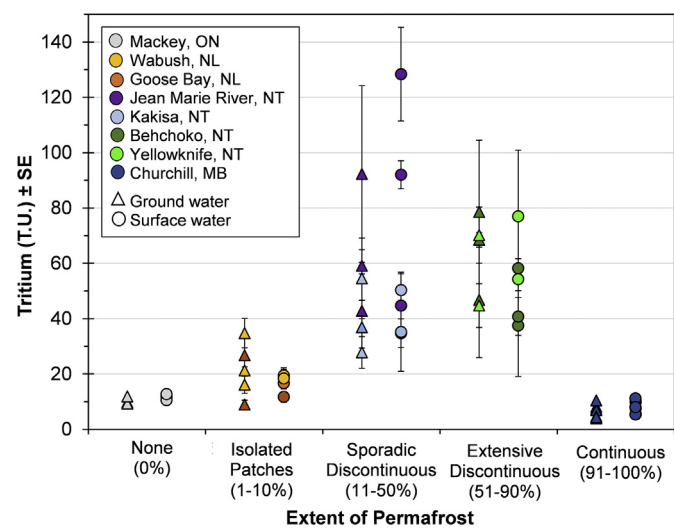


Fig. 5. Tritium concentrations in ground water discharge and surface waters in lakes located in various permafrost zones across Canada. Each sample lake is represented as a data point (surface waters = circles, groundwaters = triangles). Values in parentheses along the x-axis represent the percent of land area underlain by permafrost in the corresponding region (according to Brown et al. (2001) and NASA (2017)). Tritium data for the Ottawa River (Mackey, Ontario, no permafrost (CNL, 2017)), was included for comparison purposes. Error bars represent \pm standard error. (For interpretation of the references to colour in this figure legend, the reader is referred to the Web version of this article.)

Table 3 Pearson correlation matrix showing associations among environmental variables. Correlation coefficients (r) are presented below the diagonal and Bonferroni-adjusted p -values (to control for multiple comparisons) are presented above the diagonal. Significant correlations ($p < 0.05$) and their respective coefficients are shown in bold font.

	pH	EC	DOC	Fl ⁻	Cl ⁻	Br ⁻	NO ₃ ⁻	N ⁻	PO ₄ ³⁻	SO ₄ ²⁻	Na ⁺	NH ₄ ⁺	K ⁺	Mg ²⁺	Ca ²⁺	⁸⁷ Br	⁸⁷ Cl	HTO	MAP	MAT	Lat.
pH	0.337	0.011	0.123	0.610	0.528	0.325	< 0.001	0.071	0.535	0.618	0.576	0.174	0.036	0.863	0.009	< 0.001	0.008	< 0.001	0.003	0.022	0.915
EC	0.142	0.140	0.376	< 0.001	< 0.001	< 0.001	< 0.001	0.392	< 0.001	0.579	< 0.001	< 0.001	< 0.001	0.416	0.167	0.188	0.604	0.022	0.015	0.328	0.039
DOC	0.366	-0.216	0.313	0.194	0.142	0.614	0.613	0.566	0.169	0.573	0.028	0.164	0.364	0.934	0.041	0.001	0.015	0.001	0.015	0.022	0.035
Fl ⁻	0.226	-0.131	0.149	0.390	0.249	0.821	0.141	0.271	0.263	0.511	0.687	0.366	0.244	0.853	0.178	0.030	0.193	0.030	0.193	0.035	
Cl ⁻	0.076	0.678	-0.191	-0.127	< 0.001	0.731	0.733	0.638	0.039	< 0.001	0.623	< 0.001	0.002	< 0.001	0.864	0.581	0.284	0.896	0.140	0.212	0.752
Br ⁻	0.093	0.989	-0.215	-0.170	0.610	< 0.001	0.560	< 0.001	0.489	< 0.001	0.489	< 0.001	< 0.001	0.564	0.212	0.188	0.821	0.058	0.212	0.743	
NO ₃ ⁻	0.145	0.575	0.075	0.034	-0.051	0.614	0.000	0.482	< 0.001	0.652	< 0.001	< 0.001	0.652	< 0.001	0.674	0.925	0.853	0.471	0.523	0.550	
N ⁻	0.146	0.576	0.075	0.033	-0.051	0.615	1.000	0.483	< 0.001	0.649	< 0.001	< 0.001	0.649	< 0.001	0.670	0.924	0.850	0.468	0.522	0.546	
PO ₄ ³⁻	-0.807	-0.126	-0.202	-0.216	-0.070	-0.086	-0.104	-0.104	0.551	0.551	0.543	0.221	0.059	0.849	0.090	0.063	< 0.001	0.004	0.004	< 0.001	
SO ₄ ²⁻	0.263	0.753	-0.085	0.162	0.300	0.735	0.648	0.649	-0.153	< 0.001	0.950	< 0.001	< 0.001	0.006	0.094	0.820	0.146	0.120	0.315		
Na ⁺	0.092	0.976	-0.220	-0.165	0.530	0.995	0.662	0.664	-0.088	0.753	0.515	< 0.001	< 0.001	0.468	0.178	0.187	0.817	0.057	0.749		
NH ₄ ⁺	0.074	-0.082	0.318	0.097	-0.073	-0.102	-0.067	-0.067	0.020	0.009	-0.096	0.829	0.979	0.605	0.969	0.362	0.799	0.478	0.342	0.495	
K ⁺	0.896	-0.204	-0.060	0.315	0.921	0.761	0.762	-0.090	0.812	0.952	-0.032	< 0.001	< 0.001	0.194	0.098	0.861	0.073	0.744			
Mg ²⁺	0.199	0.931	-0.134	0.020	0.431	0.927	0.734	0.735	-0.180	0.884	0.943	0.004	0.960	0.004	0.91	0.334	0.287	0.013	0.714		
Ca ²⁺	0.304	0.673	0.003	0.304	0.673	0.578	0.372	0.372	-0.274	0.714	0.647	0.077	0.598	0.749	0.092	0.130	0.534	0.032	0.001	0.221	
⁸⁷ Br	0.026	0.120	-0.296	0.171	-0.025	0.085	0.062	0.063	-0.028	0.391	0.107	-0.006	0.191	0.238	0.246	< 0.001	0.088	0.171	0.002	0.413	
⁸⁷ Cl	-0.374	0.203	-0.449	0.028	0.082	0.184	0.014	0.014	0.248	0.198	-0.135	0.249	0.246	0.222	0.797	0.222	0.071	< 0.001	0.004	< 0.001	
HTO	0.421	-0.193	0.494	-0.158	-0.158	-0.193	0.028	-0.028	-0.270	0.034	-0.170	-0.143	-0.092	-0.249	-0.629	0.006	0.013	< 0.001	< 0.001		
MAP	-0.872	-0.077	-0.350	-0.313	-0.033	-0.107	0.760	-0.213	-0.034	-0.105	-0.277	0.140	-0.261	-0.277	-0.310	-0.201	0.263	-0.394	0.001	< 0.001	
MAT	-0.378	-0.331	0.144	-0.191	-0.216	-0.276	-0.095	0.413	-0.227	-0.277	-0.277	0.101	-0.463	-0.440	-0.505	-0.537	-0.454	0.103	-0.238		
Lat.	0.825	-0.016	0.373	0.305	-0.047	-0.049	0.088	-0.089	-0.700	0.148	-0.047	0.101	-0.048	0.054	0.180	0.121	-0.408	0.557	-0.958		

Notes: The significant correlation between $\delta^2\text{H}$ and HTO can be explained by the fact that samples highest in tritium also happened to be furthest from the nearest coast (depleted in heavy isotopes of H due to Rayleigh distillation effect), while samples taken closest to the coast (less depleted in heavy isotopes of H) also happen to be lowest in tritium ($\delta^2\text{H}$ v. distance from nearest coast (km) correlation, $r = -0.74$, $p < 0.001$, data not shown). For each correlation $n = 48$ (except for EC, Na^+ and Cl^- ($n = 46$) due to removing two outliers)

3.3. Stable isotopes

Churchill water $\delta^2\text{H}$ and $\delta^{18}\text{O}$ values varied between $-84.63\text{\textperthousand}$ and $-116.32\text{\textperthousand}$ VSMOW and $-9.48\text{\textperthousand}$ and $-15.46\text{\textperthousand}$ VSMOW, respectively. Labrador water $\delta^2\text{H}$ and $\delta^{18}\text{O}$ values were similar and ranged from $-74.51\text{\textperthousand}$ to $-112.38\text{\textperthousand}$ VSMOW and $-8.59\text{\textperthousand}$ to $-15.82\text{\textperthousand}$ VSMOW, respectively. Precipitation $\delta^2\text{H}$ and $\delta^{18}\text{O}$ values vary seasonally along the Local Meteoric Water Line (LMWL) and these results generally followed the LMWLs for Churchill ($\delta^2\text{H} = 7.52\delta^{18}\text{O} - 0.5$; $r^2 = 0.97$) and Happy Valley–Goose Bay ($\delta^2\text{H} = 7.58\delta^{18}\text{O} + 4.1$; $r^2 = 0.98$), estimated from IAEA precipitation data ([IAEA and WMO, 2017](#)), as well as the Global Meteoric Water Line ($\delta^2\text{H} = 8\delta^{18}\text{O} + 10$) described by [Craig \(1961\)](#).

$\delta^2\text{H}$ and $\delta^{18}\text{O}$ values for waters from the discontinuous permafrost zones in the Northwest Territories are depleted in heavy isotopes of hydrogen and oxygen, ranging from $-98.82\text{\textperthousand}$ to $-153.15\text{\textperthousand}$ VSMOW and $-8.72\text{\textperthousand}$ to $-18.55\text{\textperthousand}$ VSMOW, respectively (Fig. 7). These surface and groundwater samples do not fall along the LMWLs estimated for nearby Yellowknife ($\delta^2\text{H} = 6.68 \cdot \delta^{18}\text{O} - 22.1$; $r^2 = 0.95$) or Fort Smith ($\delta^2\text{H} = 6.87 \cdot \delta^{18}\text{O} - 18.0$; $r^2 = 0.96$). Meteoric waters that have undergone evaporation display systematic enrichment in both ^{18}O and ^2H , resulting in divergence from the LMWL along a Local Evaporation Line (LEL; St. Amour et al., 2005). The slope of a LEL reflects the influence of local conditions such as temperature, humidity and wind speed, integrated over the evaporation season. This is the case for the Northwest Territories surface and groundwaters, described by the LEL equation $\delta^2\text{H} = 5.27 \cdot \delta^{18}\text{O} - 53$ ($r^2 = 0.98$), as shown in Fig. 7. Also plotted in Fig. 7 are stable isotope data from northern Alberta permafrost thaw lakes extracted from Gibson et al. (2015), which fit well with the LEL estimated for the Great Slave region of the Northwest Territories. Of additional interest, waters associated with cold regions, particularly those incorporated into permafrost or glaciers, are characterized by highly depleted $\delta^2\text{H}$ and $\delta^{18}\text{O}$ signatures. Stable isotope data from permafrost studies in northern Canada (Michel, 1986; Stotler et al., 2009) are shown in Fig. 7 for comparison with the data generated in this study. Of particular interest, the most depleted (i.e., ‘ice-like’) isotopic signatures belong to lakes underlain by degrading discontinuous permafrost near Jean Marie River and Kakisa, Northwest Territories—these same lakes are also marked by the greatest enrichment of tritium (Fig. 5).

3.4. Principal components analysis

A correlation biplot of the PCA results is presented in Fig. 8. The eigenvalues for the first four PCA axes are $\lambda_1 = 0.30$, $\lambda_2 = 0.27$, $\lambda_3 = 0.12$ and $\lambda_4 = 0.08$, meaning that the first two axes of the PCA explain about 57% of the variance in the data. Axis 1 is driven mainly by Δ TEMP, LONG, LAT, pH, MAP, HTO, THAW-SENS, PO_4^{2-} and DOC, while axis 2 is driven mainly by MAGT, MAAT, EC, ELEV, Mg^{2+} , Ca^{2+} , Na^+ , Cl^- . Tritium is positively correlated with DOC, Δ TEMP and permafrost thaw sensitivity, and is associated with sporadic discontinuous and extensive discontinuous permafrost of the Taiga Plains. Alternatively, tritium is negatively correlated with the $\delta^2\text{H}$, Cl^- , Na^+ concentrations associated with the continuous permafrost of the Hudson Plains (Fig. 8).

4. Discussion

The results of this study demonstrate considerable variation in tritium activity concentrations among geographical regions and permafrost zones across Canada. These results are discussed in the context of (i) evidence for permafrost degradation, (ii) impact on water chemistry and (iii) implications for the fate and transport of tritium in the Canadian north.

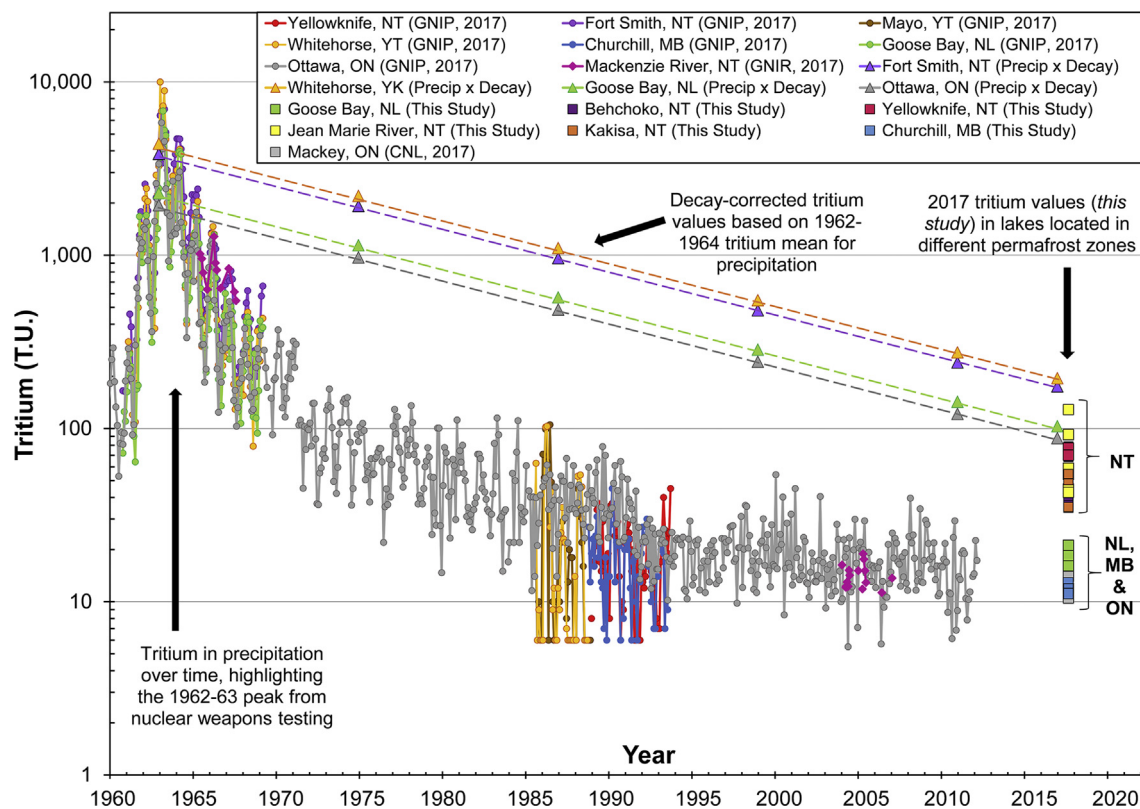


Fig. 6. Tritium trends over time. Circle markers indicate tritium concentrations in precipitation over time, showing the weapons-era peak in the early-1960s (data taken from the GNIP database, [IAEA and WMO, 2017](#)). Tritium concentrations in Mackenzie River water are shown in pink (data from GNIR database, [IAEA and WMO, 2017](#)). Triangle markers represent decay-corrected tritium values based on the 1962–1964 mean tritium values in precipitation. Square markers on the far-right represent tritium values for water samples investigated in this study. Based on tritium content, these data points group into Northwest Territories (NT) sites and the rest (Labrador [NL], Manitoba [MB] and Ontario [ON]). (For interpretation of the references to colour in this figure legend, the reader is referred to the Web version of this article.)

4.1. Evidence for permafrost thaw

Multiple lines of evidence—including tritium data, geochemical data and stable isotope data—indicate accelerated permafrost degradation in the sporadic and extensive discontinuous permafrost zones in the Canadian north. This is particularly true along the Sporadic Discontinuous–Extensive Discontinuous permafrost border in the Great Slave region of the Northwest Territories, which has warmed by over 2.5 °C over the past 60 years (Fig. 1) and has also experienced elevated forest fire activity. Tritium concentrations in study lakes in this region are enriched, ranging from 37 to 92 T.U. in groundwaters and 35–128 T.U. in surface waters (Fig. 5), indicating that they are fed in part by permafrost meltwater. Nearby Great Slave Lake, one of the largest freshwater lakes in the world, had tritium concentrations of 39 T.U. in near-shore surface water and 31 T.U. in shoreline groundwater seepage (Table 2). Tritium concentrations in precipitation in this region (Fort Smith and Yellowknife, NT) peaked with atmospheric weapons-testing at about 7000 T.U. in 1963 and have declined exponentially since that time, reaching about 7–40 T.U. by 1993 (current precipitation in the region contains less than 25 T.U.). Likewise, tritium concentrations in the Mackenzie River (the major drainage feature in the region) reached 1280 T.U. in 1966 and declined to 11 T.U. by 2006 (Fig. 6).

It is not surprising that the highest tritium concentrations observed in this study were from sites in the western Great Slave Lake region, as several other recent studies have pointed to rapid permafrost degradation in this region (e.g., Quinton et al., 2011; Quinton and Baltzer, 2013; Calmels et al., 2015; Gibson et al., 2015; Hickman, 2016). A number of other studies have pointed to increased streamflows (St. Jacques and Sauchyn, 2009; Connon et al., 2014), increased organic carbon liberation (Rouse et al., 1997; Vonk et al., 2015; Hickman, 2016;

Tank et al., 2016; Fouché et al., 2017) and increased mercury concentrations in some surface waters and fish (Carrie et al., 2009; Gordon et al., 2016; Reyes, 2016) in this part of the country, which are likely related to permafrost degradation. While permafrost thaw occurs to varying degrees throughout the Arctic and sub-Arctic, it is the southern boundary of permafrost where the rates of thaw are the greatest (Throop et al., 2012; Quinton and Baltzer, 2013). Approximately 30–65% of permafrost on the southern margins of the discontinuous zone in north-western Canada has degraded over the last century (Beilman and Robinson, 2003), with rates of degradation increasing in recent decades (e.g., Quinton and Baltzer, 2013; Chadburn et al., 2017), resulting in the southern permafrost boundary migrating north by about 120 km between 1964 and 1990 (Kwong and Gan, 1994).

In addition to increasing global temperatures, changing wildfire dynamics accelerate permafrost degradation (Jafarov et al., 2013; Smith et al., 2015; Gibson, 2017) and may help explain elevated tritium concentrations in the discontinuous permafrost zone of the Mackenzie River Valley. Canadian empirical models of fire frequency and severity suggest that average area burned per decade will double by 2050 and will increase on the order of 3.5–5.5 times by 2100 due to a warmer and drier climate (Balshi et al., 2009). The 2014 forest fire season in the Northwest Territories was the worst in three decades, with more than 380 fires burning a record 3.4 million hectares (Darwent, 2016), including large fires near the regions sampled in this study (Behchoko, Jean Marie River and Kakisa). Indeed, a recent study by Gibson (2017) in the Taiga Plains west of Great Slave Lake found that wildfire has been responsible for about 25% of permafrost thaw over the past 30 years. These recent wildfires may have contributed to the permafrost thaw process, resulting in increased environmental mobility of tritium in the region.

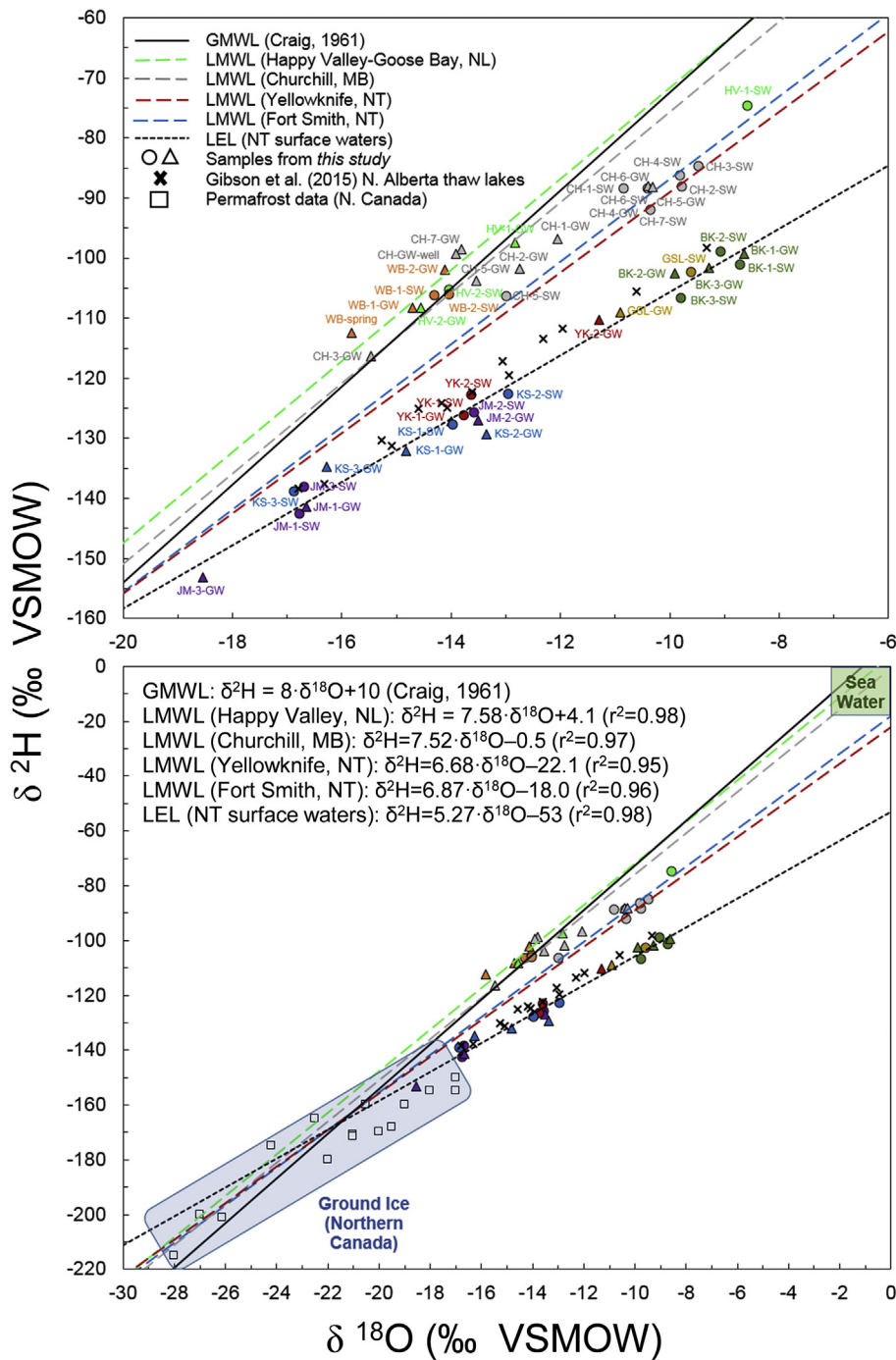


Fig. 7. Stable isotope signatures for the groundwater and surface water samples. Isotope signatures from waterbodies identified as permafrost thaw lakes in northern Alberta from Gibson et al. (2015) and values from permafrost studies in northern Canada (Michel, 1986, 2011; Stotler et al., 2009) are included for comparison. Also included are the Local Meteoric Water Lines (LMWL) for Happy Valley–Goose Bay, Churchill, Fort Smith and Yellowknife (data extracted from IAEA and WMO (2017) database), the Local Evaporation Line (LEL) for surface waters at the Northwest Territories sites and the Global Meteoric Water Line (GMWL). Note the differences in scale between top and bottom figures.

Quinton and Baltzer (2013) studied permafrost condition near Scotty Creek in the Liard River Valley (located about 50 km to the west of Jean Marie River within the discontinuous permafrost zone) and found that permafrost has degraded substantially over the past two decades, with permafrost depth decreasing from about 42 m to 24 m between 1998 and 2010, and the active layer depth (summer thaw depth) increasing from about 0.55 m to 0.92 m over the same period. Likewise, studies of permafrost integrity in the Jean Marie River First Nation traditional territory (1702 km²) by Calmels et al. (2015) found that peat-rich permafrost is present in about 52% of the area, with 36% of that permafrost at a high level of vulnerability and 16% at a medium level of vulnerability to thaw. Ekali (JM-1), Sanguez (JM-2) and Gargan (JM-3) lakes, which contained the highest tritium content in both

groundwater seepage and surface waters in our study (~43–128 T.U.; Figs. 4 and 5), are surrounded by permafrost that is at either high or medium vulnerability to thaw (Calmels et al., 2015). Groundwater seepage and surface waters in Ekali and Sanguez lakes also showed the most depleted δ¹⁸O values (−16.7 to −18.6‰) observed in this study (Fig. 7), suggesting that these lakes are sourced in part by cold, ice-like waters (Jouzel et al., 1994; Clark and Fritz, 1997; Michel, 1986, 2011; Stotler et al., 2009; Henkemans et al., 2018). In a study of frost-blister ice in the North Fork Pass, Yukon, Michel (1986) reported tritium values as high as 161 T.U. (decay-corrected to November 2017 = 25 T.U.) in spring waters on extensive discontinuous permafrost, which was considerably higher than local precipitation at the time so these values were attributed to weapons-test era precipitation.

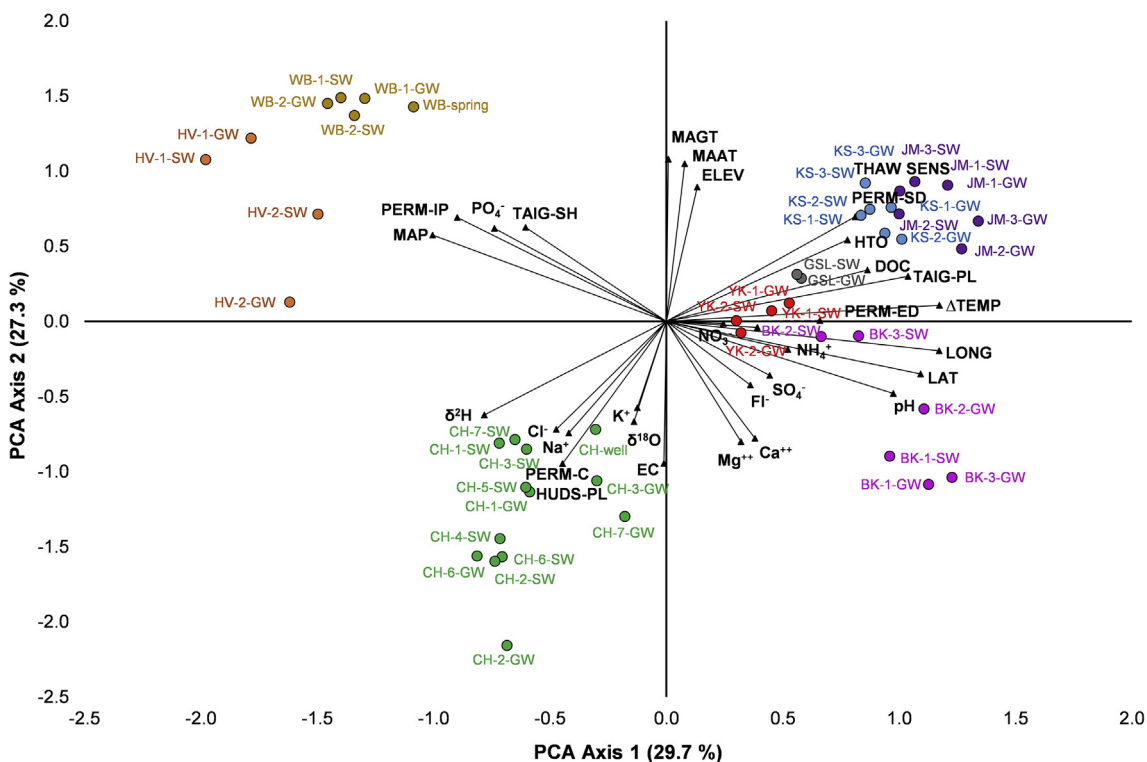


Fig. 8. PCA biplot of the physical, chemical and environmental variables for the study lakes, illustrating the approximate correlations and relative gradient lengths of the environmental variables. Study lakes are colour-coded by region. (For interpretation of the references to colour in this figure legend, the reader is referred to the Web version of this article.)

Tritium measurements were consistently low (< 12 TU.) in all of the lakes around Churchill, in both surface waters and groundwater seepage (Figs. 3–5). Stotler et al. (2009) assessed tritium concentrations near Lupin, Nunavut within the continuous permafrost zone and reported that concentrations ranged from 14 to 21 TU. in surface waters—slightly higher than our Churchill lakes but similar to the Labrador lakes (Fig. 3). The low-lying landscape of the Churchill region also floods frequently during the spring freshet (as it did several months prior to sampling in 2017), which may have brought waters lower in tritium from farther south and flushed surface waters to Hudson Bay, thereby increasing hydrodynamic dispersion of tritiated waters. As shown by Camill (2005), permafrost degradation in northern Manitoba's continuous permafrost zone near Churchill is minimal compared to degradation in the discontinuous and sporadic zones to the south or in the western Arctic. This conclusion is supported by a permafrost hydrology study (Déry et al., 2005) which shows decreasing annual flows for rivers discharging into Hudson Bay and the Labrador Sea (i.e., northern Manitoba and Labrador sites), in contrast with the increasing river flows observed in the Northwest Territories' Mackenzie River basin (Walvoord and Striegl, 2007; St. Jacques and Sauchyn, 2009; Connon et al., 2014). The main cause of these recent increases in streamflow in the central Mackenzie River basin is likely a broadscale and recent mobilization of subsurface water (i.e., melting permafrost) coupled with enhanced infiltration and deeper flow paths (Smith et al., 2007; Walvoord and Striegl, 2007; St. Jacques and Sauchyn, 2009; Connon et al., 2014).

The $\delta^2\text{H}$ and $\delta^{18}\text{O}$ values for surface- and ground-water samples from Churchill and Labrador study regions (Fig. 7) correlate reasonably well with the local meteoric water lines and local precipitation is regarded as the source of water for these regions. Alternatively, the $\delta^2\text{H}$ and $\delta^{18}\text{O}$ values for surface- and ground-waters from the Northwest Territories study locations (Yellowknife, Behchoko, Jean Marie River, Kakisa and Great Slave Lake) are depleted in $\delta^2\text{H}$ relative to the Local Meteoric Water Lines for Yellowknife and Fort Smith. When plotted

along the derived LEL for the Great Slave region ($\delta^2\text{H} = 5.27\delta^{18}\text{O} - 53$), our values correlate well with other reported stable isotopic signatures for surface waters for the Canadian western Arctic (St. Amour et al., 2005; Gibson et al., 2015). This local depletion of $\delta^2\text{H}$ may be due to the fact that much of the water that enters the Great Slave Lake basin, which acts like a large sponge, is recycled several times before leaving as water vapour or as discharge to the Arctic Ocean (Woo and Thorne, 2003), with each evaporation event resulting in isotopic depletion. This also suggests that it would take longer for HTO to be flushed from the Great Slave Lake basin compared to environments with shorter water residence times.

As described by Jouzel et al. (1994), the relative abundance of the various stable isotopes of oxygen and hydrogen in precipitation fluctuates seasonally, with summer precipitation typically enriched in the heavier isotopes relative to winter precipitation. In cold and dry northern regions, air becomes progressively depleted in ^{18}O and enriched in ^{16}O , meaning that precipitation that forms most glacial and permafrost ice is also depleted in ^{18}O . As permafrost melts, it would be expected that meltwater would be rich in ^{16}O and depleted in ^{18}O . Indeed, the isotopic signatures for the lakes with the highest tritium content (i.e., JM-1, JM-2 and JM-3) were also the most depleted in both $\delta^{18}\text{O}$ and $\delta^2\text{H}$ (Fig. 7). Stable isotope values for surface- and ground-waters at these locations were similar to the depleted isotopic signatures of permafrost and glacial ice from northern Canada (Michel, 1986, 2011; Stotler et al., 2009), providing further evidence that these lakes are fed by permafrost meltwater. Gibson et al. (2015) studied water isotopes in permafrost thaw lakes in northern Alberta and report that lakes fed by permafrost meltwater do not have a distinctive $\delta^{18}\text{O}$ or $\delta^2\text{H}$ signature compared to non-thaw lakes, but melt lakes do tend to be less evaporatively-enriched than other lakes and have higher water yields due largely to higher rates of flushing attributed to throughput of meltwater. Indeed, water isotope data from Gibson et al. (2015) fit well with the isotope data reported in this study (Fig. 7).

4.2. Impact on water chemistry

Several researchers have noted that other contaminants, such as mercury, have also been increasing in lakes within the Jean Marie River region. For example, mercury concentrations in predatory fish has increased considerably since the mid-1990s in Ekali, Sanguez and Gargan lakes leading to fish consumption advisories (Evans et al., 2005; Government of the Northwest Territories, 2016, 2018), which can have major implications for nearby residents who rely on wild fish as a large proportion of their diet (Calmels et al., 2015; Reyes, 2016). One of the characteristics of peat-rich permafrost is the potential for it to have high accumulation and concentration of metals such as mercury (Smieja-Król et al., 2010), meaning that melting permafrost may be a potential source of mercury contamination in these lakes, as observed in Swedish sub-Arctic lakes (Klaminder et al., 2008; Rydberg et al., 2010). Of course, these mercury dynamics are also strongly related to reduced sulfur in organic-rich peat. Schuster et al. (2018) recently determined that permafrost regions contain twice as much mercury as the rest of all other soils, the atmosphere and oceans combined. The tritium results reported in this study, which show significantly enriched tritium concentrations in these three lakes, support that these mercury-enriched Jean Marie River-area lakes are sourced in part by thawing permafrost.

Thawing permafrost can also impact the water chemistry of receiving wetlands, lakes and rivers (Vonk et al., 2015; Roberts et al., 2017; Colombo et al., 2018). As the active layer deepens and more hydrological flow pathways develop in the permafrost, increased geochemical weathering, mobilization and transport of materials that were previously frozen in permafrost will occur (Kokelj et al., 2005). The geochemical and isotopic signatures of the study lakes provide further evidence of extensive permafrost degradation in the Great Slave Lake region of the Northwest Territories. As hypothesized, groundwater seepage discharging to lake shorelines was typically enriched in ions associated with weathering processes (Cl^- , K^+ , Na^+ , Mg^{2+} , Ca^{2+}) relative to ambient surface waters, and tritium concentrations in the study thaw-lakes are positively correlated with DOC concentrations (Table 3). Likewise, Roberts et al. (2017) found that permafrost thaw in the Canadian Arctic has resulted in increased ionic concentrations in lakes receiving meltwater, with Ca^{2+} , Cl^- and SO_4^{2-} concentrations increasing substantially since 2008 due to increased solute-rich meltwater inputs, while melting of permafrost and deepening of the active layer have been associated with increased particulate and DOC transport to Arctic lakes and rivers (Prowse et al., 2006; Xu et al., 2009). Further, analysis of the Mackenzie River basin, where all of our Northwest Territories sites marked by enriched tritium are located, has shown a 39% increase in DOC export from the Mackenzie River basin (Tank et al., 2016).

4.3. Implications for tritium fate and transport

Since the Nuclear Test-ban Treaty in 1963, the exponential decline in tritium concentration in surface waters is due to a combination of factors including radioactive decay and mixing/dilution (hydrodynamic dispersion), as described by Clark and Fritz (1997). However, as shown by the precipitation decay-curves in Fig. 6, the persistence of tritium in the environment is increased substantially if the weapons-era precipitation is virtually frozen in place (e.g., incorporation into permafrost/glaciers or deposited in a region with a long water residence time) and subject to only minimal hydrodynamic dispersion in addition to radioactive decay. For example, tritium concentrations in most surface waters in Canada had declined exponentially to less than 30 TU. by 1990 owing to mixing and decay processes (Clark and Fritz, 1997). However, if hydrodynamic dispersion is removed from the equation, it would take the same waters until the year 2040–2060 (an additional 50 + years) to decline to 30 TU. by radioactive decay alone (determined by extrapolating decay curves in Fig. 6 and determining their intersection with the water concentration curves). Similar tritium

trends have been observed in glacier cores (Koerner and Taniguchi, 1976; Kotzer et al., 2000; Clark et al., 2007; Wu et al., 2010; Van der Wel et al., 2011; Kang et al., 2015) and glacial or ground ice meltwater (Michel, 1986; Blais et al., 2001; Kang et al., 2015).

Observations of enriched tritium concentrations measured in thaw lakes on a regional scale within the discontinuous permafrost zone in the Northwest Territories cannot be explained unless these lakes are fed by sources containing a high proportion of precipitation from the 1960s–1970s period (Clark and Fritz, 1997; Gibson et al., 2015). This is attributed to thaw of frozen permafrost that had incorporated and sequestered a high proportion of 1960s precipitation, as decay-corrected 1961–1967 precipitation from Fort Smith and Whitehorse peak tritium values from permafrost and ice core literature are statistically indistinguishable from tritium concentrations in the thaw lakes included in this study (Fig. 3). To put the tritium values presented in this study into context, pre-1950s concentrations of tritium were about 2–8 TU. (UNSCEAR, 1993), while present-day concentrations are typically in the 16–25 TU. range in waterbodies across Canada (CNSC, 2009). Concentrations in Lake Ontario and Lake Huron, which have nuclear power stations along their shores resulting in ongoing tritium releases, are approximately 40–60 TU. (CNSC, 2009). In terms of ecological and human health, the maximum tritium concentration reported in this study comprises less than 2% of the Canadian drinking water guideline of 7000 Bq L^{-1} (60,000 TU.; CNSC, 2009).

Gibson et al. (2015) measured tritium in permafrost thaw fed lakes in northern Alberta, located about 200–500 km south of our Northwest Territories study lakes, and found tritium concentrations in the range of about 11–20 TU., which were elevated relative to nearby non-thaw lakes, but significantly lower than our Northwest Territories sites located farther north (Fig. 3). Northern Alberta study lakes were located in the sporadic discontinuous and isolated patches of permafrost, while the lakes included in our study were located in the extensive discontinuous and sporadic discontinuous permafrost zones. Based on historical precipitation data (IAEA and WMO, 2017) and the relatively close proximity of the Gibson et al. (2015) northern Alberta lakes to Northwest Territories study lakes, it can be assumed that they received similar tritium loads from atmospheric fallout during the weapons-test era (Figs. 1b and 6) and radioactive decay is constant. Thus, the significantly higher tritium in present-day surface and groundwaters (Fig. 3) must be due to differences in hydrodynamic dispersion of weapons-era tritiated precipitation (Clark and Fritz, 1997), based on local permafrost characteristics and corresponding hydrology. In permafrost zones, small increases in ground temperature can correspond to large changes in water storage and runoff pathways (Rouse et al., 1997). Interestingly, tritium levels in northern Alberta thaw-lakes (Gibson et al., 2015) fall within the range of isolated patches of permafrost near Labrador's Wabush and Happy Valley–Goose Bay (Fig. 3), implying that the Labrador sites have experienced similar hydrodynamic dispersion over the past half-century.

The nature of a permafrost environment calls into question the possibility of isotopic fractionation due to the freeze–thaw cycles experienced by permafrost and active layer waters. Freeze-out fractionation occurs as water freezes due to diffusion kinetics (Throckmorton et al., 2016), with the heavier isotopes of hydrogen (^3H and ^2H) and oxygen (^{18}O) preferentially incorporated into the solid ice phase during freezing, while the residual liquid becomes isotopically depleted of the heavy isotopes (Michel, 1986). Because the ^3H atom has three times the mass of ^1H atom and one-and-a-half times the mass of a ^2H atom, the magnitude of fractionation for tritium in the ice–water system should be larger than the deuterium fractionation (Michel, 1986), which may help explain the enriched tritium concentrations observed in this study. Waters that experience frequent freeze–thaw cycles, such as active layer waters with a long residence time, may become enriched in tritium due to this fractionation process.

The $\delta^2\text{H}$ value of ice in isotopic equilibrium with water has been estimated to be between 17‰ and 20.6‰ more positive than the water

in freshwater systems at natural freezing rates (Suzuki and Kimura, 1973; Gibson and Prowse, 1999). As shown in Fig. 7, $\delta^2\text{H}$ values for the surface and groundwater samples are isotopically depleted relative to local meteoric waters, particularly for the Northwest Territories discontinuous permafrost samples (JM, KS, YK, BK), which may indicate freeze-out fractionation, as freeze-out and evaporation fractionation are isotopically indistinguishable (Throckmorton et al., 2016). Michel (1986) suggests that due to the low concentration of tritium in most waters, this freeze-out isotopic fractionation for tritium may not be detectable. In a study of isotope geochemistry of ground ice in the Yukon, Michel (1986) detected isotopic fractionation of $\delta^{18}\text{O}$ and $\delta^2\text{H}$, but could not detect these fractionation effects in tritium data (with values up to 200 TU.). Since our water melt-water samples contained a maximum of 128 TU., or 128 ^3H atoms per 10^{18} atoms of ^1H , it is possible that any fractionation effects would be masked by measurement error, as reported by Michel (1986). Furthermore, Gibson et al. (2015) suggest that evaporation is expected to have only a minor enrichment effect on tritium content in lakes, which they estimate to be in the range of 0.8 TU. for the most enriched lakes.

The observed positive correlation between DOC and HTO in waters in the discontinuous permafrost zone also has implications for tritium fate and transport, as this may indicate that dissolved and/or particulate OBT can be liberated from aged biomass together with HTO from aged ice. This is particularly relevant given the more frequent wildfires in the north which de-stabilize previously immobile organic matter. Unfortunately, the mass of the sample filtrate was insufficient for OBT analysis, so quantification of OBT in these systems was not possible.

5. Conclusions

The Arctic and sub-Arctic tundra constitutes the largest terrestrial sink for radioactive contaminants on earth (AMAP, 2011). Tritium is likely the most widespread anthropogenic radionuclide in the Arctic, yet there is virtually no specific information on the mobility and bioavailability of tritium in arctic ecosystems (IRSN, 2010). This is likely because the combination of low temperatures, the lack of mobile water and high levels of organic material has led to the Arctic being perceived as a low-mobility stable sink term for anthropogenic radionuclides (AMAP, 2011). A warming climate, however, will upset these assumptions and will likely result in altered behaviour of radionuclides in the Arctic and sub-Arctic (McEwen and de Marsily, 1991). For example, Kipp et al. (2018) recently investigated possible sources to help explain increases in radium-228 in the Arctic Ocean and attributed thawing permafrost—and the associated liberation of radium from melting permafrost and subsequent fluxes to the Mackenzie River and eventually the ocean—as a contributing source.

The results presented in this study demonstrate increased tritium mobility in the Arctic and sub-Arctic environment—at concentrations higher than expected—as a result of a warming climate. Changes in the physicochemical status of the sub-Arctic environment related to the levels and nature of organic matter and carbon, runoff events, and nature of vegetation all have direct bearing on the environmental behaviour of radionuclides in the northern environment (AMAP, 2011). Increased frequency and severity of wildfires may also accelerate permafrost thaw, resulting in increased environmental mobility of tritium in the region. Our results show that this effect is most pronounced in the discontinuous permafrost zones in the Great Slave region of the Northwest Territories, with significantly enriched tritium content in surface waters and groundwaters in this region. Regions that have experienced minimal permafrost thaw to date (typically in the continuous permafrost zone) are generally low in surface water tritium; however, it is anticipated that as these regions continue to warm in the future, surface waters may become enriched in tritium. These results are useful for better understanding the impacts of climate change on the north and better understanding the environmental fate and transport of tritium.

Tritium anomalies may provide insight about the age of permafrost

melt sources and can be used as an effective tool when paired with stable isotope analysis for better understanding environmental change in the north. Further, a better understanding of the cycling of tritium and other radionuclides that are highly mobile in the environment will improve our understanding of Arctic radioecology under new environmental conditions. Thaw lakes that are enriched in HTO also provide a unique opportunity to study organically bound tritium (OBT) dynamics and environmental partitioning, particularly the role that liberated DOC plays (Kim et al., 2013; Eyrolle-Boyer et al., 2014; Eyrolle et al., 2018). Better understanding of watersheds that have already completely thawed, as well as close monitoring of watersheds that are yet to thaw, will also provide valuable information.

6. Author agreement/declaration

All authors have seen and approved the final version of the manuscript being submitted. This manuscript is the authors' original work, has not received prior publication and is not under consideration for publication elsewhere.

Conflicts of interest

No conflicts of interest to declare.

7. Funding source declaration

This study was funded by the Government of Canada through Atomic Energy of Canada Limited's Federal Science and Technology program (project FST-51400.05, Fate and Transport Models for Predicting Environmental Radioactivity in Northern Ecosystems).

Acknowledgements

We thank the Aurora Research Institute for their assistance in obtaining a research license for sample collection in the Northwest Territories (License # 15928), and the Dehcho First Nation and the communities of Fort Providence, Enterprise, Jean Marie River, Churchill, Wabush and Happy Valley-Goose Bay for their support. We also thank LeeAnn Fishback and staff at the Churchill Northern Studies Centre for assistance with logistics and sample collection, as well as for providing a research permit for sample collection within the Churchill Wildlife Management Area. We thank Heather Rousselle, Mike Bredlaw, Sang Bog Kim and Todd Chaput for conducting tritium and ion analysis. Lastly, we thank Lars Brinkmann, David Rowan and Karen Sharp for assistance with interpretation of data, and Sang Bog Kim, Vlad Korolevych, Jesse Carrie, Jennifer Olfert, Joanne Ball and three anonymous referees for reviewing this manuscript.

Appendix A. Supplementary data

Supplementary data related to this article can be found at <https://doi.org/10.1016/j.jenvrad.2018.07.006>.

References

- Aarkrog, A., 1994. Radioactivity in polar regions—main sources. *J. Environ. Radioact.* 25, 21–35.
- Aggarwal, P., 2016. IAEA, isotopes and water resources management. In: IAEA Cooperation Products in Fukushima Prefecture, June 2016, Fukushima Prefecture.
- AMAP (Arctic Monitoring and Assessment Programme), 2011. In: Kallenborn, R. (Ed.), Combined Effects of Selected Pollutants and Climate Change in the Arctic Environment, AMAP Technical Report No. 5, Oslo. 108 pp.
- AMAP (Arctic Monitoring and Assessment Programme), 2017. Snow, water, ice and permafrost in the arctic (SWIPA). In: Arctic Monitoring and Assessment Programme, Oslo, Norway, 269 pp.
- Åkerman, H.J., Johansson, M., 2008. Thawing permafrost and thicker active layers in Sub-arctic Sweden. *Permafrost and Periglacial Processes* 19, 279–292.
- Anisimov, O., Renneva, S., 2006. Permafrost and changing climate: the Russian perspective. *Ambio* 35, 169–175.

Balshi, M.S., McGuire, A.D., Duffy, P., Flannigan, M., et al., 2009. Assessing the response of area burned to changing climate in western boreal North America using a Multivariate Adaptive Regression Splines (MARS) approach. *Glob. Change Biol.* 15, 578–600.

Banks, W.S.L., Paylor, R.L., Hughes, W.B., 1996. Using thermal-infrared imagery to delineate ground-water discharge. *Ground Water* 34, 434–443.

Barrie, L.A., Gregor, D., Hargrave, B., Lake, R., et al., 1992. Arctic contaminants: sources, occurrence and pathways. *Sci. Total Environ.* 122, 1–74.

Beilman, D.W., Robinson, S.D., 2003. Peatland permafrost thaw and landform type along a climate gradient. In: In: Phillips, M. (Ed.), *Proceedings of the Eighth International Conference on Permafrost*, vol. 1. pp. 61–65.

Blais, J.M., Schindler, D.W., Muir, D.C.G., Sharp, M., et al., 2001. Melting glaciers: a major source of persistent organochlorines to subalpine Bow Lake in Banff National Park, Canada. *Ambio* 30, 410–415.

Bouchard, F., MacDonald, L.A., Turner, K.W., Thienpont, J.R., et al., 2017. Paleolimnology of thermokarst lakes: a window into permafrost landscape evolution. *Arctic Science* 3, 91–117.

Brown, J., Ferrians Jr., O.J., Heginbottom, J.A., Melnikov, E.S., 2001. Circum-Arctic map of permafrost and ground-ice conditions. In: National Snow and Ice Data Center/World Data Center for Glaciology. Digital Media, Boulder, Colorado, USA available at: <http://nsidc.org>.

Brown, R.J.E., 1970. *Permafrost in Canada: its influence on northern development*. In: *Natural Resource Council of Canada*. University of Toronto Press, Toronto, Ontario, Canada 246 pp.

Burn, C.R., Michel, F.A., 1988. Evidence for recent temperature-induced water migration into permafrost from the tritium content of ground ice near Mayo, Yukon Territory, Canada. *Can. J. Earth Sci.* 25, 909–915.

Calmels, F., Delisle, G., Allard, M., 2008. Internal structure and the thermal and hydrological regime of a typical lithalsa: significance for permafrost growth and decay. *Can. J. Earth Sci.* 45, 31–43.

Calmels, F., Laurent, C., Pivot, F., Ireland, M., 2015. How Permafrost Thaw May Impact Food Security of Jean Marie River First Nation. NWT. Extended abstract, GEOQuebec 2015, September 20–23 2015, Quebec City, Canada.

Camill, P., 2005. Permafrost thaw accelerates in Boreal peatlands during late-20th century climate warming. *Clim. Change* 68, 135–152.

Carrie, J., Wang, F., Sanei, H., Macdonald, R.W., et al., 2009. Increasing contaminant burdens in an Arctic fish (*Lota lota*) in a warming climate. *Environ. Sci. Technol.* 44, 316–322.

Chadburn, S.E., Burke, E.J., Cox, P.M., Friedlingstein, P., et al., 2017. An observation-based constraint on permafrost loss as a function of global warming. *Nat. Clim. Change* 7, 340–344.

Christensen, T.R., Johansson, T., Åkerman, H.J., Mastepanov, M., et al., 2004. Thawing sub-arctic permafrost: effects on vegetation and methane emissions. *Geophys. Res. Lett.* 31, L04501.

Chizhov, A.B., Dereviagin, A.Y., 1998. Tritium in Siberian permafrost. In: *Proceedings of the Seventh International Permafrost Conference*, Yellowknife, Northwest Territories, Canada, pp. 151–158.

Clark, I.D., Henderson, L., Chappellaz, J., Fisher, D., et al., 2007. CO₂ isotopes as tracers of firn air diffusion and age in an Arctic ice cap with summer melting, Devon Island, Canada. *J. Geophys. Res.* 112, D01301.

Clark, I.D., Fritz, P., 1997. *Environmental Isotopes in Hydrogeology*. CRC Press/Lewis Publishers, Boca Raton, FL, USA.

CNSC (Canadian Nuclear Safety Commission), 2009. Tritium Releases and Dose Consequences in Canada in 2006, Part of the Tritium Studies Project. INFO-0793. 39 pp.

Colombo, N., Salerno, F., Gruber, S., Freppaz, M., et al., 2018. Review: impacts of permafrost degradation on inorganic chemistry of surface fresh water. *Glob. Planet. Change* 162, 69–83.

Connon, R.F., Quinton, W.L., Craig, J.R., Hayashi, M., 2014. Changing hydrologic connectivity due to permafrost thaw in the lower Liard River valley, NWT, Canada. *Hydrolog. Proc.* 28, 4163–4178.

CNL (Canadian Nuclear Laboratories), 2017. Annual Safety Report–environmental Monitoring in 2016 at Chalk River Laboratories. CRL-509243-ASR-2016.

Craig, M., 1961. Isotopic variation in meteoric waters. *Science* 133, 1702–1703.

Danby, R.K., Hik, D.S., 2007. Evidence of recent treeline dynamics in southwest Yukon from aerial photographs. *Arctic* 60, 411–420.

Darwent, R., 2016. Fire severity in the 2014 Northwest Territories fires. In: *Nat. Resour. Can., Can. for. Serv., North. for. Cent.*, Edmonton, AB. Insights, No. 4b.

deGroot, P.A., 2004. *Handbook of Stable Isotope Analytical Techniques*, vol. 1. Elsevier, pp. 1–37 (Chapter 1).

Déry, S.J., Stieglitz, M., McKenna, E.C., Wood, E.F., 2005. Characteristics and trends of river discharge into Hudson, James and Ungava Bays, 1964–2000. *J. Clim* 18, 2540–2557.

Dredge, L.A., 1992. *Field Guide to the Churchill Region, Manitoba*. Geological Survey of Canada, miscellaneous report no. 53. 52 pp.

Dyke, L.D., 2001. Contaminant migration through the permafrost active layer, Mackenzie Delta area, Northwest Territories, Canada. *Polar Rec.* 37, 215–228.

Environment Canada, 2017. Historical Climate Database. Available at: <http://climate.weather.gc.ca/> (last accessed: 17 January 2018).

Evans, M.S., Lockhart, L., Doetzel, L., Low, G., et al., 2005. Elevated mercury concentrations in fish in lakes in the Mackenzie River Basin: the role of physical, chemical, and biological factors. *Sci. Total Environ.* 351–352, 479–500.

Eyrille, F., Ducros, L., Le Dizès, S., Beaugelin-Seiller, K., Charmasson, S., et al., 2018. An updated review on tritium in the environment. *J. Environ. Radioact.* 181, 128–137.

Eyrille-Boyer, F., Boyer, P., Claval, D., Charmasson, S., Cossionnet, C., 2014. Apparent enrichment of organically bound tritium in rivers explained by the heritage of our past. *J. Environ. Radioact.* 136, 162–168.

Fortier, D., Allard, M., Shur, Y., 2007. Observation of rapid drainage system development by thermal erosion of ice wedges on Bylot Island, Canadian Arctic Archipelago. *Permafrost. Periglac.* Process 18, 229–243.

Fouché, J., Lafrenière, M.J., Rutherford, K., Lamoureux, S., 2017. Seasonal hydrology and permafrost disturbance impacts on dissolved organic matter composition in high Arctic catchments. *Arctic Science* 3, 378–405.

Gibson, C., 2017. *Long Term Effects of Wildfire on Permafrost Stability and Carbon Cycling in Northern Peatlands*. M.Sc. thesis. University of Alberta 98 p.

Gibson, J.J., Birks, S.J., Yi, Y., 2015. Higher tritium concentrations measured in permafrost thaw lakes in northern Alberta. *Hydrolog. Process* 30, 245–249.

Gibson, J.J., Prowse, T.D., 1999. Isotopic characteristics of ice cover in a large northern river basin. *Hydrolog. Process* 13, 2537–2548.

Gordon, J., Quinton, W., Branfireun, B.A., Olefeldt, D., 2016. Mercury and methylmercury biogeochemistry in a thawing permafrost wetland complex, Northwest Territories, Canada. *Hydrolog. Process* 30, 3627–3638.

Government of Canada, 2015. *The Science of Climate Change*. 24 pp. Available at: <https://www.canada.ca/en/environment-climate-change/services/climate-change/science.html> (last accessed: 14 January 2018).

Government of the Northwest Territories, 2016. Department of environment and natural resources. Northwest Territories cumulative impact monitoring program (NWT CIMP). In: *Monitoring and Research Results, 2010–2015: Fish*, 37 pp.

Government of the Northwest Territories, 2018. Fish Consumption Guidance, Dehcho Region. Department of Health and Social Services Available online: <http://www.hss.gov.ca/en/services/fish-consumption-guidance/site-specific-fish-consumption-advice> (last accessed: 06 February 2018)ss.

Grannas, A.M., Bogdal, C., Hageman, K.J., Halsall, C., et al., 2013. The role of the global cryosphere in the fate of organic contaminants. *Atmospheric Chem. Phys.* 13, 3271–3305.

Grosse, G., Goetz, S., McGuire, A.D., Romanovsky, V.E., Schuur, E.A.G., 2016. Changing permafrost in a warming world and feedbacks to the Earth system. *Environ. Res. Lett.* 11, 040201.

Hammer, Ø., Harper, D.A.T., Ryan, P.D., 2001. *PAST: paleontological statistics software package for education and data analysis*. *Palaeontologia Electronica* 4, 1–9.

Heginbottom, J.A., Dubreuil, M.A., Harker, P.A., 1995. Canada permafrost. In: *Nat. Resour. Can.*, Ottawa, ON, Canada, 5th ed. National Atlas of Canada.

Henkemans, E., Frapé, S., Ruskeeniemi, T., Anderson, N.J., Hobbs, M., 2018. A landscape-isotopic approach to the geochemical characterization of lakes in the Kangerlussuaq region, west Greenland. *Arct. Antarct. Alp. Res.* 50, S100018.

Hickman, J.L., 2016. *Seasonal Evolution of Active Layer Formation in Subarctic Peat Plateaux and Implications for Dissolved Organic Matter Composition and Transfer*. MSc thesis. Wilfrid Laurier University, Waterloo, Ontario, Canada 185 pp.

IAEA (International Atomic Energy Agency)/WMO (World Meteorological Organization), 2017. Global Network of Isotopes in Precipitation (GNIP) and Global Network of Isotopes in Rivers (GNIR). Available at: <http://www.iaea.org/water> (last accessed: 21 December 2017).

IRSN (L'Institut de Radioprotection et de Sûreté Nucléaire), 2010. Radionuclide Fact Sheet: Tritium and the Environment. 26 pp.

Jafarov, E.E., Romanovsky, V.E., Genet, H., McGuire, A.D., Marchenko, S.S., 2013. The effects of fire on the thermal stability of permafrost in lowland and upland black spruce forests of interior Alaska in a changing climate. *Environ. Res. Lett.* 8, 035030.

Jeffries, M.O., Krouse, H.R., Shakur, M.A., Harris, S.A., 1984. Isotope geochemistry of stratified lake "a", Ellesmere Island, N.W.T., Canada. *Can. J. Earth Sci.* 21, 1008–1017.

Jorgenson, M.T., Shur, Y.L., Pullman, E.R., 2012. Abrupt increase in permafrost degradation in Arctic Alaska. *Geophys. Res. Lett.* 33, L02503.

Jouzel, J., Koster, R.D., Suozzo, R.J., Russell, G.L., 1994. Stable water isotope behavior during the last glacial maximum: a general circulation model analysis. *J. Geophys. Res.* 99, 25791–25802.

Judge, A., 1973. The prediction of permafrost thickness. *Can. Geotech. J.* 10, 1–11.

Kang, S., Wang, F., Morgenstern, U., Zhang, Y., et al., 2015. Dramatic loss of glacier accumulation area on the Tibetan Plateau revealed by ice core tritium and mercury records. *The Cryosphere* 9, 1213–1222.

Kazemi, G.A., Lehr, J.H., Perrochet, P., 2006. *Groundwater Age*. John Wiley & Sons, Inc. 325 p.

Kim, S.B., Baglan, N., Davis, P.A., 2013. Current understanding of organically bound tritium (OBT) in the environment. *J. Environ. Radioact.* 126, 83–91.

Kipp, L.E., Charette, M.A., Moore, W.S., Henderson, P.B., et al., 2018. Increased fluxes of shelf-derived materials to the central Arctic Ocean. *Sci. Adv.* <https://doi.org/10.1126/sciadv.aoa1302>.

Klaminder, J., Hammarlund, D., Kokfelt, U., Vonk, J.E., Bigler, C., 2010. Lead contamination of subarctic lakes and its response to reduced atmospheric fallout: can the recovery process be counteracted by the ongoing climate change? *Environ. Sci. Technol.* 7, 2335–2340.

Klaminder, J., Yoo, K., Rydberg, J., Giesler, R., 2008. An explorative study of mercury export from a thawing palsu mire. *J. Geophys. Res. Biogeosci.* 113, 1–9.

Koerner, R.M., Taniguchi, H., 1976. Artificial radioactivity layers in the Devon Island ice cap, Northwest Territories. *Can. J. Earth Sci.* 13, 1251–1255.

Kokelj, S.V., Burn, C.R., 2005. Geochemistry of the active layer and near-surface permafrost, Mackenzie delta region, Northwest Territories, Canada. *Can. J. Earth Sci.* 42, 37–48.

Kokelj, S.V., Jenkins, R.E., Milburn, D., Burn, C.R., Snow, N., 2005. The influence of thermokarst disturbance on the water quality of small upland lakes, Mackenzie Delta region, Northwest Territories, Canada. *Permafrost. Periglac.* Process 16, 343–353.

Kotzer, T.G., Kudo, A., Zheng, J., Workman, W., 2000. Natural and anthropogenic levels of tritium in a Canadian Arctic ice core, Agassiz Ice Cap, Ellesmere Island, and

comparison with other radionuclides. *J. Glaciol.* 46, 35–40.

Kwong, J., Gan, T., 1994. Northward migration of permafrost along the Mackenzie Highway and climate warming. *Clim. Change* 26, 399–419.

Lee, D.R., Cherry, J.A., 1979. A field exercise on groundwater flow using seepage meters and mini-piezometers. *Journal of Geological Education* 27, 6–10.

McEwen, T., de Marsily, G., 1991. The Potential Significance of Permafrost on the Behaviour of a Deep Radioactive Waste Repository. Swedish Nuclear Power Inspectorate SKI technical report 91: 8. 63 pp.

Michel, F.A., 1986. Isotope geochemistry of frost-blister ice, North Fork pass, Yukon, Canada. *Can. J. Earth Sci.* 23, 543–549.

Michel, F.A., 2011. Isotope characterization of ground ice in northern Canada. *Permafrost Periglac.* Process 22, 3–12.

Michel, F.A., Fritz, P., 1978. Environmental isotopes in permafrost related waters along the Mackenzie Valley corridor. In: *Proc. 3rd Int. Conf. on Permafrost, Natl. Res. Council Canada, vol. 1.* pp. 207–211.

NASA (National Aeronautics and Space Administration), 2017. Earth Observatory Program, Map Produced by J. Stevens Using Data from the National Snow and Ice Data Center. Available at: <https://visibleearth.nasa.gov/view.php?id=87794> (last accessed: 10 November 2017).

Payette, S., Delwaide, A., Caccianiga, M., Beauchemin, M., 2004. Accelerated thawing of subarctic peatland permafrost over the last 50 years. *Geophys. Res. Lett.* 31, L18208.

Payette, S., Rochefort, L. (Eds.), 2001. *Écologie des tourbières du Québec-Labrador. Presse de l'Université Laval, Québec, Québec, Canada* 644 pp.

Prowse, T.D., Wrona, F.J., Reist, J.D., Gibson, J.J., et al., 2006. Climate change effects on hydroecology of Arctic freshwater ecosystems. *Ambio* 35, 347–358.

Quinn, G.P., Keough, M.J., 2002. *Experimental Design and Data Analysis for Biologists. Cambridge University Press, New York* 537 pp.

Quinton, W.L., Baltzer, J.L., 2013. The active-layer hydrology of a peat plateau with thawing permafrost (Scotty Creek, Canada). *Hydrogeol. J.* 21, 201–220.

Quinton, W.L., Hayashi, M., Chasmer, L.E., 2011. Permafrost-thaw-induced land cover change in the Canadian subarctic: implications for water resources. *Hydrol. Process.* 25, 152–158.

Reyes, E.S., 2016. Assessing the Risks for the Optimization of Nutrient Benefits from Wild-harvested Fish Consumption in the Northwest Territories, Canada. MSc thesis. University of Waterloo, Waterloo, Ontario, Canada 107 pp.

Riley, J.L., Notzl, L., Greene, R., 2013. Labrador nature atlas. In: *Ecozones, Ecoregions and Ecodistricts. Nature Conservancy of Canada, Toronto, Ontario.* vol. II 127 pp.

Roberts, K.E., Lamoureux, S.F., Kyser, T.K., Muir, D.G.C., et al., 2017. Climate and permafrost effects on the chemistry and ecosystems of high Arctic lakes. *Sci. Rep.* 7, 13292.

Rouse, W.R., Douglas, M.V., Hecky, R.E., Hershey, A.E., et al., 1997. Effects of climate change on the freshwaters of Arctic and subarctic North America. *Hydrol. Process.* 11, 873–902.

Rowland, J.C., Jones, C.E., Altmann, G., Bryan, R., et al., 2010. Arctic landscapes in transition: responses to thawing permafrost. *Eos. Trans. AGU* 91, 229–230.

Rydberg, J., Klaminder, J., Rosén, P., Bindler, R., 2010. Climate driven release of carbon and mercury from permafrost mires increases mercury loading to sub-arctic lakes. *Sci. Total Environ.* 408, 4778–4783.

Schindler, D.W., Smol, J.P., 2006. Cumulative effects of climate warming and other human activities on freshwaters of Arctic and subarctic North America. *Ambio* 35, 160–198.

Schuster, P.F., Schaefer, K.M., Aiken, G., Antweiler, R.C., et al., 2018. Permafrost stores a globally significant amount of mercury. *Geophys. Res. Lett.* 45, 1–9.

Shur, Y., Hinkel, K.M., Nelson, F.E., 2005. The transient layer implication for geocryology and climate-change science. *Permafrost Periglac.* Process 16, 5–17.

Smieja-Król, B., Fialkiewicz-Koziel, B., Sikorski, J., Palowski, B., 2010. Heavy metal behavior in peat—a mineralogical perspective. *Sci. Total Environ.* 408, 5924–5931.

Smith, L.C., Pavelsky, T.M., MacDonald, G.M., Shiklomanov, A.I., Lammers, R.B., 2007. Rising minimum daily flows in northern Eurasian rivers: a growing influence of groundwater in the high-latitude hydrologic cycle. *J. Geophys. Res.* 112, G04S47.

Smith, S., 2011. Trends in Permafrost Conditions and Ecology in Northern Canada. Canadian Biodiversity: Ecosystem Status and Trends 2010, Technical Thematic Report No. 9. Canadian Councils of Resource Ministers, Ottawa, ON iii + 22 p.

Smith, M.W., Burgess, M.M., 2004. Sensitivity of permafrost to climate warming in Canada. *Geological Survey of Canada, Bulletin* 579 24 p.

Smith, S.L., Riseborough, D.W., Bonnavenport, P.P., 2015. Eighteen year record of forest fire effects on ground thermal regimes and permafrost in the central Mackenzie Valley, NWT, Canada. *Permafrost Periglac.* Process 26, 289–303.

Smith, S.L., Romanovsky, V.E., Lewkowicz, A.G., Burn, C.R., et al., 2010. Thermal state of permafrost in north America—A contribution to the international polar year. *Permafrost Periglac.* Process 21, 117–135.

Smith, S.L., Wolfe, S.A., Riseborough, D.W., Nixon, F.M., 2009. Active-layer characteristics and summer climatic indices, Mackenzie valley, Northwest Territories, Canada. *Permafrost Periglac.* Process 20, 201–220.

St. Amour, N.A., Gibson, J.J., Edwards, T.W.D., Prowse, T.D., Pietroniro, A., 2005. Isotopic time-series partitioning of streamflow components in wetland-dominated catchments, lower Liard River basin, Northwest Territories, Canada. *Hydrol. Process.* 19, 3357–3381.

St Jacques, J.-M., Sauchyn, D.J., 2009. Increasing winter baseflow and mean annual streamflow from possible permafrost thawing in the Northwest Territories, Canada. *Geophys. Res. Lett.* 36, L01401.

Stotler, R.L., Frape, S.K., Ruskeeniemi, T., Ahonen, L., et al., 2009. Hydrogeochemistry of groundwaters in and below the base of thick permafrost at Lupin, Nunavut, Canada. *J. Hydrol.* 373, 80–95.

Suzuki, T., Kimura, T., 1973. D/H and $^{18}\text{O}/^{16}\text{O}$ fractionation in the ice-water system. *Mass Spectroscopy* 21, 229–233.

Tank, D.E., Striegl, R.G., McClelland, J.W., Kokelj, S.V., 2016. Multi-decadal increases in dissolved organic carbon and alkalinity flux from the Mackenzie drainage basin to the Arctic Ocean. *Environ. Res. Lett.* 11 054015.

Throckmorton, H.M., Newman, B.D., Heikoop, J.M., et al., 2016. Active layer hydrology in an arctic tundra ecosystem: quantifying water sources and cycling using water stable isotopes. *Hydrol. Process.* 30, 4972–4986.

Throop, J., Lewkowicz, A.G., Smith, S.L., 2012. Climate and ground temperature relations at sites across the continuous and discontinuous permafrost zones, Northern Canada. *Can. J. Earth Sci.* 49, 865–876.

UNSCEAR, 1993. *Sources, Effects and Risks of Ionizing Radiation: Report to the UN General Assembly with Appendices. United Nations, New York.*

Van der Wel, L.G., Streurman, H.J., Isaksson, E., Helsen, M.M., et al., 2011. Using high-resolution tritium profiles to quantify the effects of melt on two Spitsbergen ice cores. *J. Glaciol.* 57, 1087–1097.

Vonk, J.E., Tank, S.E., Bowden, W.B., Laurion, I., et al., 2015. Reviews and syntheses: effects of permafrost thaw on Arctic aquatic ecosystems. *Biogeosciences* 12, 7129–7167.

Walvoord, M.A., Striegl, R.G., 2007. Increased groundwater to stream discharge from permafrost thawing in the Yukon River basin: potential impacts on lateral export of carbon and nitrogen. *Geophys. Res. Lett.* 34, L12402.

Wang, W., Wu, T., Zhao, L., Li, R., et al., 2018. Exploring the ground ice recharge near permafrost table on the central Qinghai-Tibet Plateau using chemical and isotopic data. *J. Hydrol.* 560, 220–229.

Way, R.G., Lewkowicz, A.G., 2016. Modelling the spatial distribution of permafrost in Labrador-Ungava using the temperature at the top of permafrost. *Can. J. Earth Sci.* 53, 1010–1028.

Woo, M., 2012. *Permafrost Hydrology. Springer-Verlag Berlin Heidelberg* 564 p.

Woo, M., Kane, D., Carey, S., Yang, D., 2008. Progress in permafrost hydrology in the new millennium. *Permafrost Periglac.* Process 19, 237–254.

Woo, M., Thorne, R., 2003. Streamflow in the Mackenzie basin, Canada. *Arctic* 56, 328–340.

Wu, Q., Zhang, T., Liu, Y., 2010. Permafrost temperatures and thickness on the Qinghai-Tibet plateau. *Glob. Planet. Change* 72, 32–38.

Xu, C., Guo, L., Ping, C., White, D.M., 2009. Chemical and isotopic characterization of size-fractionated organic matter from cryoturbated tundra soils, northern Alaska. *J. Geophys. Res.* 114, G03002.